



Radar Remote Sensing and Polarimetry

Paul A. Rosen
Jet Propulsion Laboratory
California Institute of Technology

July 15, 2013



Acknowledgements

Much of the the material in the lecture was drawn from materials collaboratively developed with Dr. Scott Hensley at JPL.



Overview

- What is radar remote sensing?
 - Remote sensing problems, phenomenology, and radar solutions
- Radar observables, emphasizing polarimetry
- Example observing systems and applications

What is Remote Sensing?

From Wikipedia:

Remote sensing is the acquisition of information about an object or phenomenon, without making physical contact with the object.





What is Remote Sensing?

In modern usage, **Remote sensing** generally refers to the use of aerial [or satellite] sensor technologies to detect and classify objects on Earth [or other planets] (both on the surface, and in the atmosphere and oceans) by means of propagated signals (e.g. electromagnetic radiation emitted from aircraft or satellites).

- Active
 - Radar, sonar, lidar...
- Passive
 - Multi/hyperspectral, photometers, radiometers, gravity sensors, field detectors, seismometers...
- Technique and sensor choice depends on what information is desired and the required accuracy and resolution for that information.



Why Radar Remote Sensing?

- Why Remote Sensing?
 - Area too large, inaccessible or hazardous for *in situ* observation
 - Sensitive to aspects of the environment that elude our senses
 - Efficient, quantitative monitoring of changes to the environment either from natural or anthropogenic causes
- Why Radar Remote Sensing?
 - We control the source, so we can select what we observe
 - Sees through clouds
 - Sees at night
 - Sensitive to the geometric and electrical properties of objects rather than chemical constituents

What do we want to measure?

- Topography
- Geography
- Chemistry
 - Composition
 - Phase
- Dynamics
 - Thermo-
 - Hydro-
 - Geo-
 - Bio-

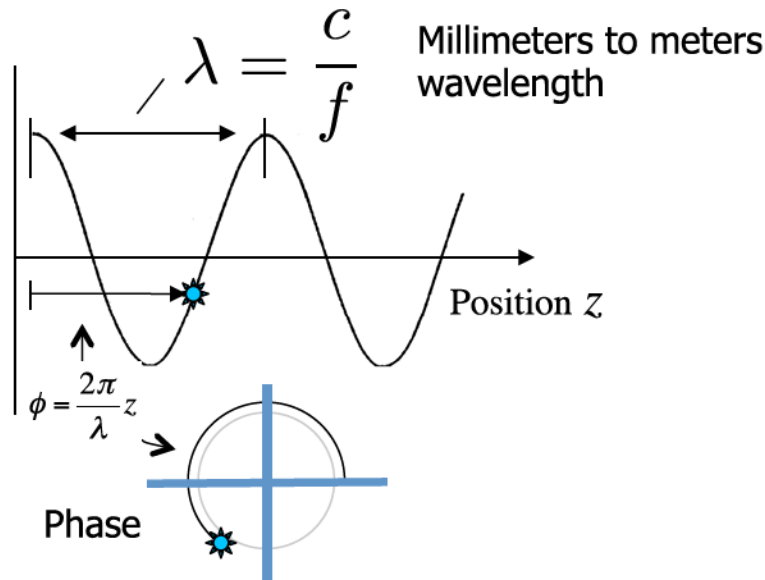




Radar Remote Sensing

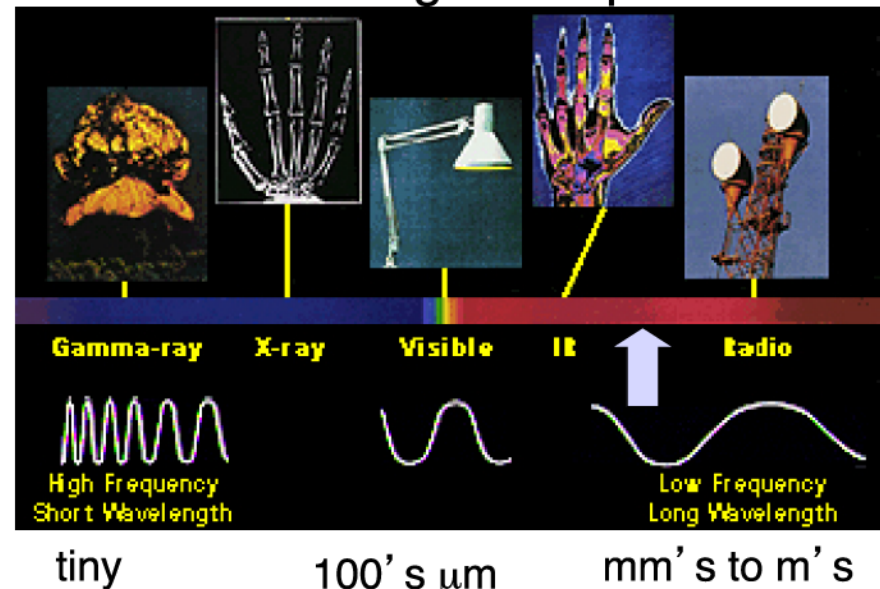
- Radar is an *active* remote sensing technique – we provide the illumination source and control its characteristics
 - > Transmitted Energy — greater power gives a larger reflection, implying greater detectability (when not speckle limited)
 - > Received Energy — larger antenna gives more received energy, implying greater detectability (when not speckle limited)
 - > Frequency (wavelength) — radar is most sensitive to objects larger than 1/10 of the radar wavelength. Electrical properties of objects change depending on their material composition and on the wavelength
 - > Phase – a phase-stable radar allows aperture synthesis for image formation and interferometry for differential metrology
 - > Polarization — gives sensitivity to the orientation and shape of objects as well as their electrical properties
 - > Resolution — gives ability to discriminate between/resolve objects and control coverage
 - > Coverage — through the physical pattern of the radiated energy and design of the entire radar/flight system, we can determine area coverage rate

Radar and Light Waves



- Radars operate at microwave frequencies, an invisible part of the electromagnetic spectrum
- Microwaves have wavelengths in the millimeter to meter range
- Like lasers, radars are coherent; we can determine the signal's phase

The Electromagnetic Spectrum

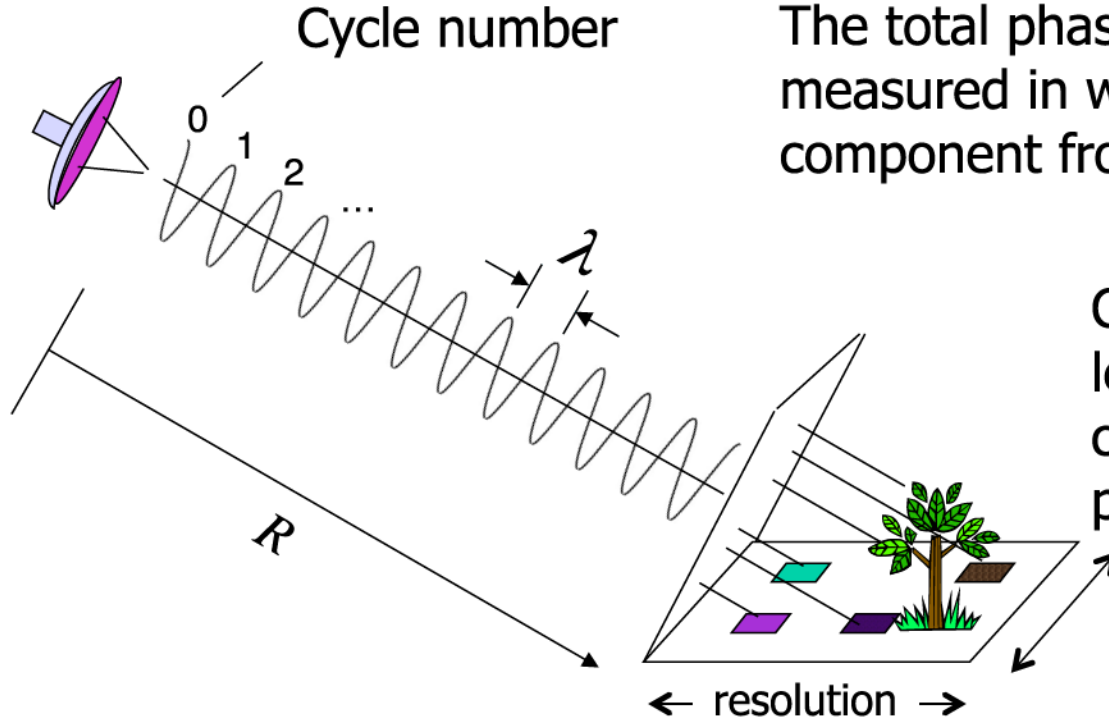


Common Radar Frequency Bands

Band	Ka	Ku	X	C	S	L	P
Wavelength (cm)	1	2	3	6	12	24	75
Frequency (G-cycles/s)	30	15	10	5	2.5	1.2	0.4

Radar Design Features – Phenomenology Perspective

The radar view of the surface depends on the design features of the radar – its wavelength, polarization, resolution, and phase characteristics

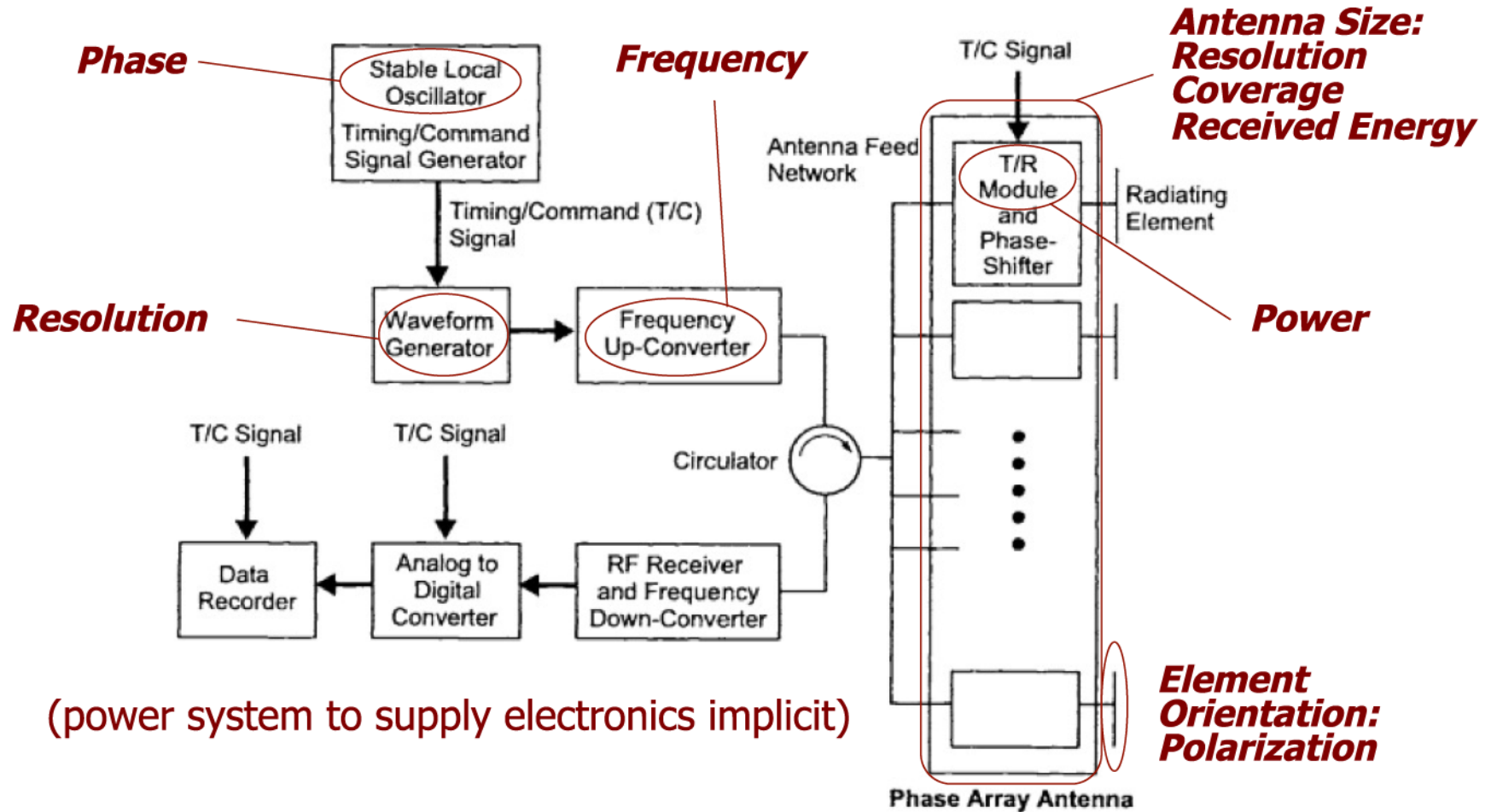


The total phase is two-way range measured in wave cycles + random component from the surface

Collection of random path lengths and scatterer contributions jumbles the phase of the echo

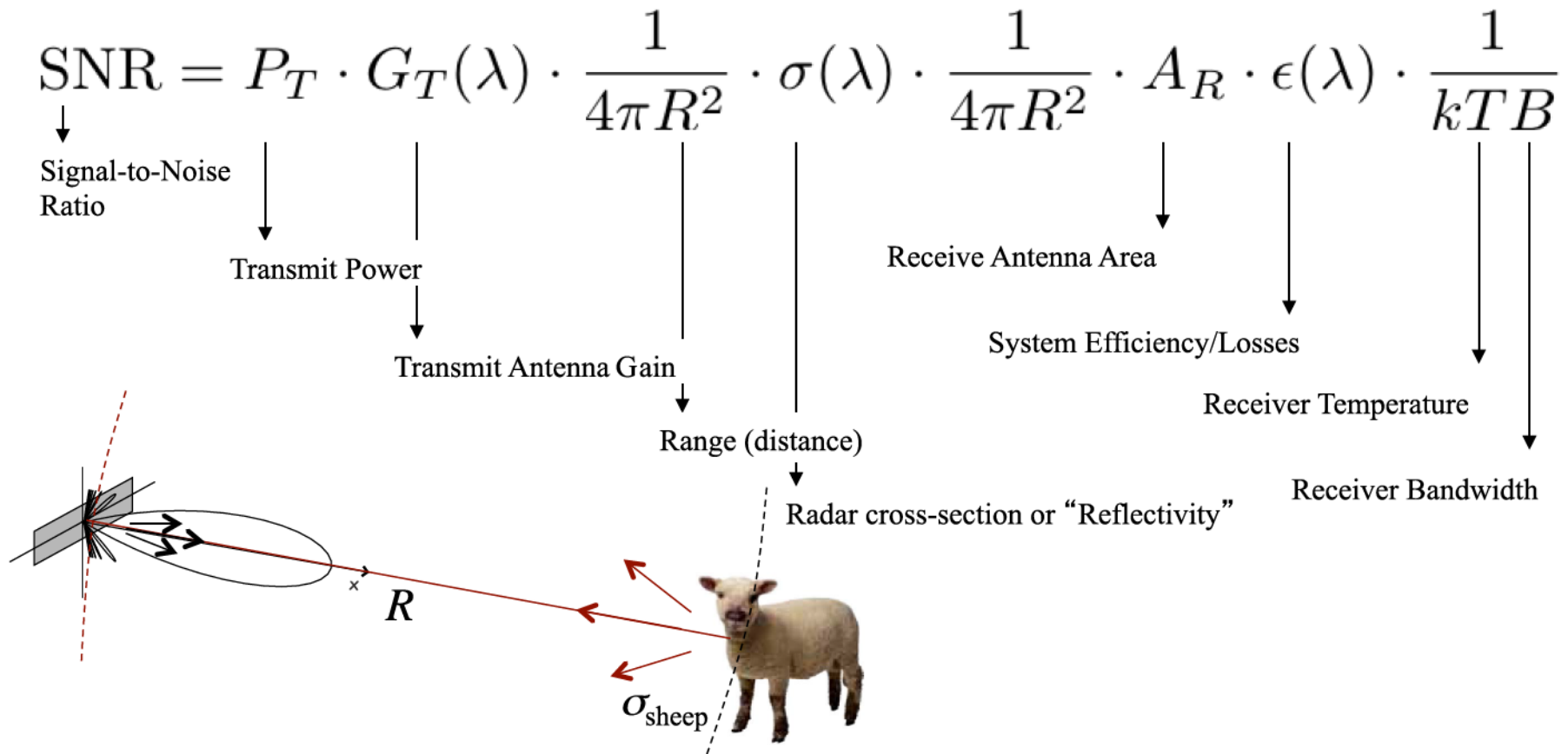


Radar Design Features – Hardware Perspective



Radar Remote Sensing Trade Space

- Sensitivity of the measurement determined by “radar equation”



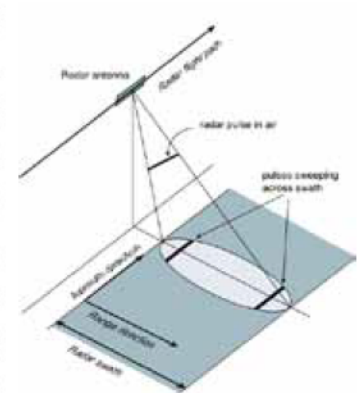
Sample Calculation for Radar Equation

TABLE I
NOMINAL ERS-1 RADAR SYSTEM PARAMETERS

Parameter	ERS-1 value
Wavelength, m	0.0566
Peak power, watts	4800
Pulse rate, Hz	1679 nominal
Pulse length, μ sec	37.1
Antenna length, m	10.0
Antenna width, m	1.0
Antenna gain, dB	43.2
Range bandwidth, MHz	15.55
Receiver noise temperature, K	3700
Integrated Sidelobe ratio, dB	-14
Quantization Noise (5 bit), dB	-30
Slant range resolution, m	10.2
Ground range resolution, m	25
Azimuth resolution, m	6
Orbit altitude, km	790
Incidence angle, deg	24
Orbit repeat interval, days	3, 35, 165

TABLE II
ERS-1 RADAR DESIGN CONTROL TABLE

Parameter	ERS-1 value in dB/dBW
Peak power	36.8
Antenna directional gain	45.9
Antenna efficiency	-3
$\frac{1}{4\pi}$	-11
$\frac{1}{R^2}$	-118.6
Illuminated area	78.4
σ^0	-14
$\frac{1}{4\pi}$	-11
$\frac{1}{R^2}$	-118.6
Antenna area	10
Antenna efficiency	-3
System losses	-3
Oversampling gain	1.8
Total	-109.3
Thermal noise (kTB)	-121.0
Signal to noise ratio	11.7



From "Accuracy of Topographic Maps Derived from ERS-1 Interferometric Radar", Zebker et al (1994), TGARSS

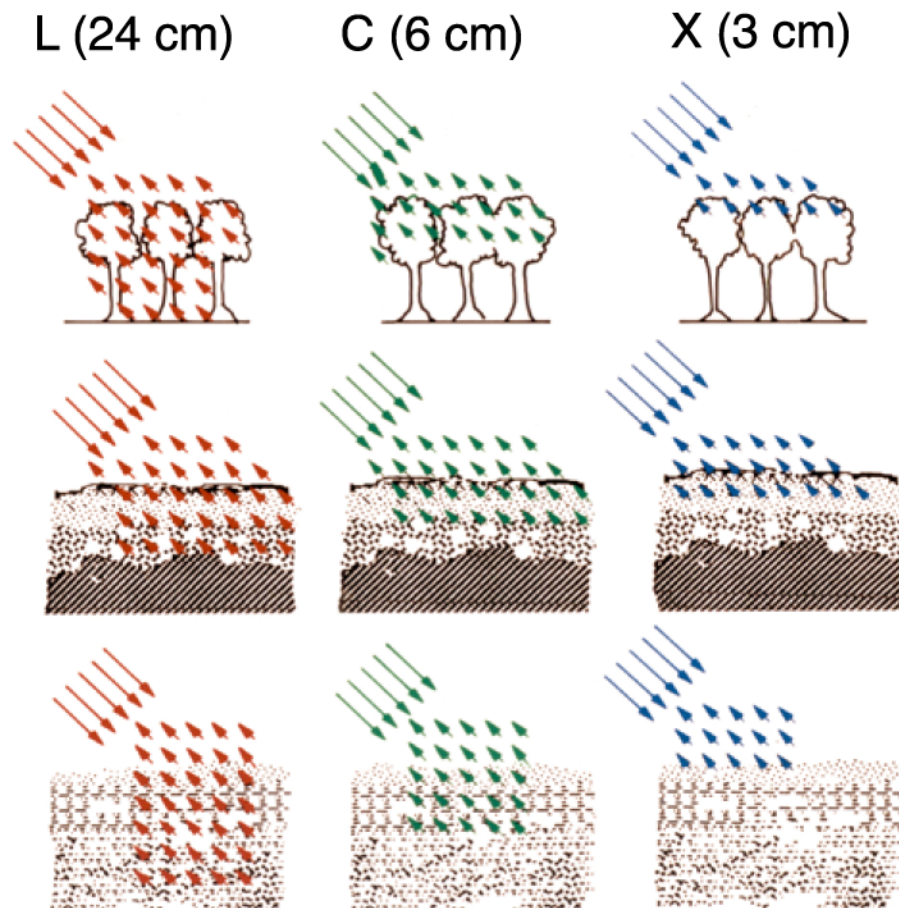
Wavelengths—a Measure of Surface Scale Sizes

Light interacts most strongly with objects on the size of the wavelength.

Forest: Leaves reflect X-band wavelengths but not L-band.

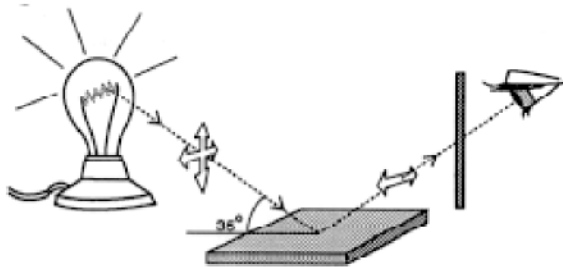
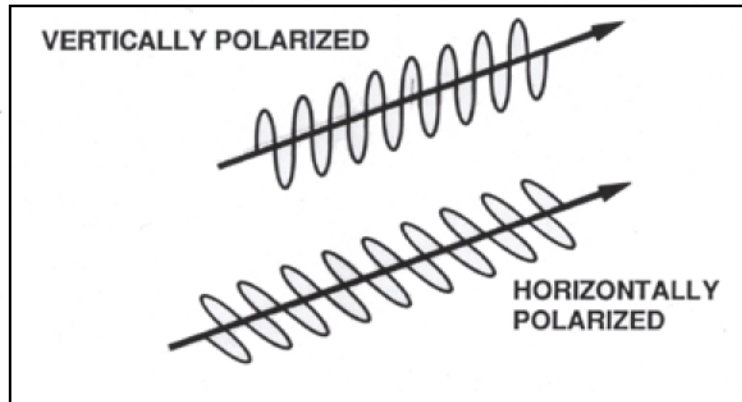
Dry soils: The surface looks rough to X-band but not L-band.

Ice: The surface and layering look rough to X-band but not L-band.



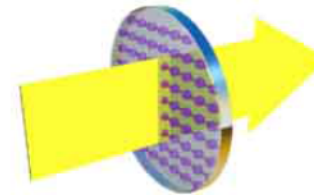
Polarization—A Measure of Surface Orientations and Properties

Wave Polarization

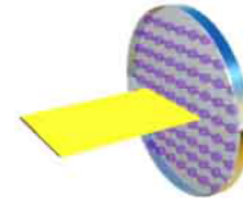


Mostly horizontal polarization is reflected from a flat surface.

Polarization Filters



Vertical polarization passes through horizontally arranged absorbers.

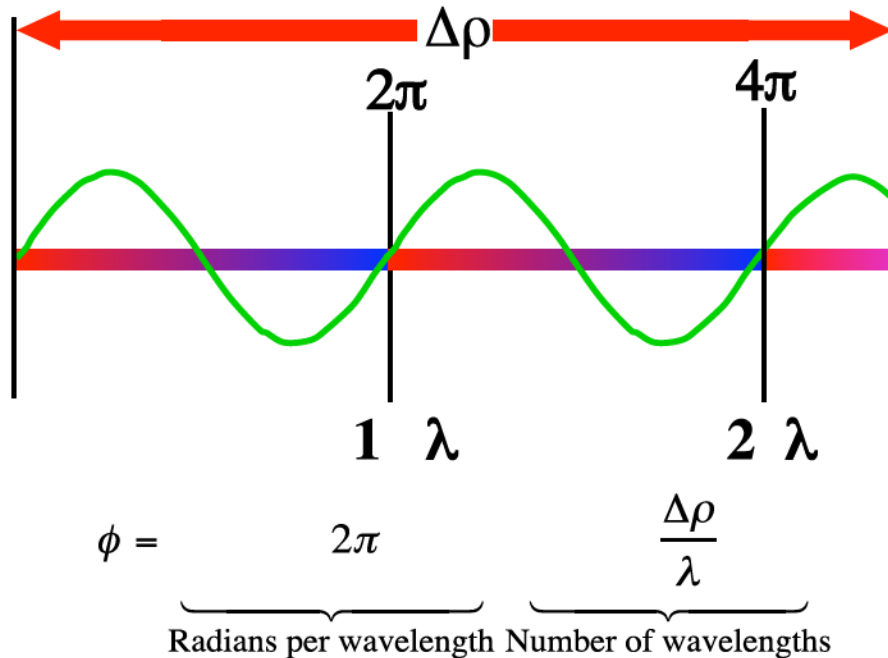


Horizontal polarization does not pass through horizontally arranged absorbers.

Color figures from www.colorado.edu/physics/2000

Phase and Radar Interferometry

- Interferometric phase is simply another means of measuring distance. Traditional stereoscopic measurement of the “parallax,” or relative displacement an object has from two stereo images, is proportional to the height of the object and the separation between the two imaging points
- For SAR systems, the parallax is the range difference from a point to the two observation antennas



- Phase measurements in interferometric systems can be made with degree-level accuracy, and with typical radar wavelengths in 3-80 cm range this corresponds to parallax measurements having millimeter accuracy



Common Types of Remote Sensing Radar Sensors

Altimeters determine the height of a surface by measuring the round trip time it takes for a radar signal to reflect from the surface to determine surface elevation

Sounders/Profilers measure the reflected power in a volume over range

Scatterometers measure the magnitude of the backscattered reflected energy from the surface in the radar beam. The backscatter is related to both the surface composition, through the dielectric constant, and to the surface roughness at the wavelength scale

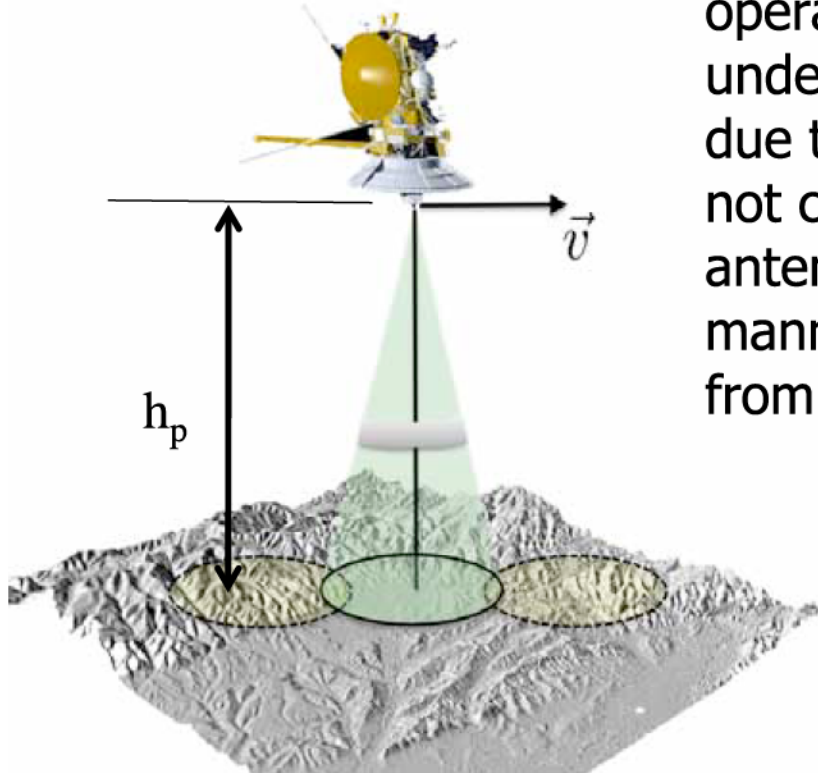
Synthetic Aperture Radar (SAR) Imagers generate fine resolution backscatter imagery, using the motion of the platform to synthesize a long antenna

Polarimeters generate backscatter measurements from multiple polarizations. Polarimetric information helps distinguish surface roughness from surface composition effects on the backscatter

Interferometers: interferometric systems generally require fine resolution, hence are SAR systems. Data collected from different vantage points determine topographic information. In interferometric systems the parallax is typically much less than a pixel so the topographic information is obtained from a phase measurement that makes highly accurate parallax measurements possible. These phase measurements are then converted into elevation measurements.

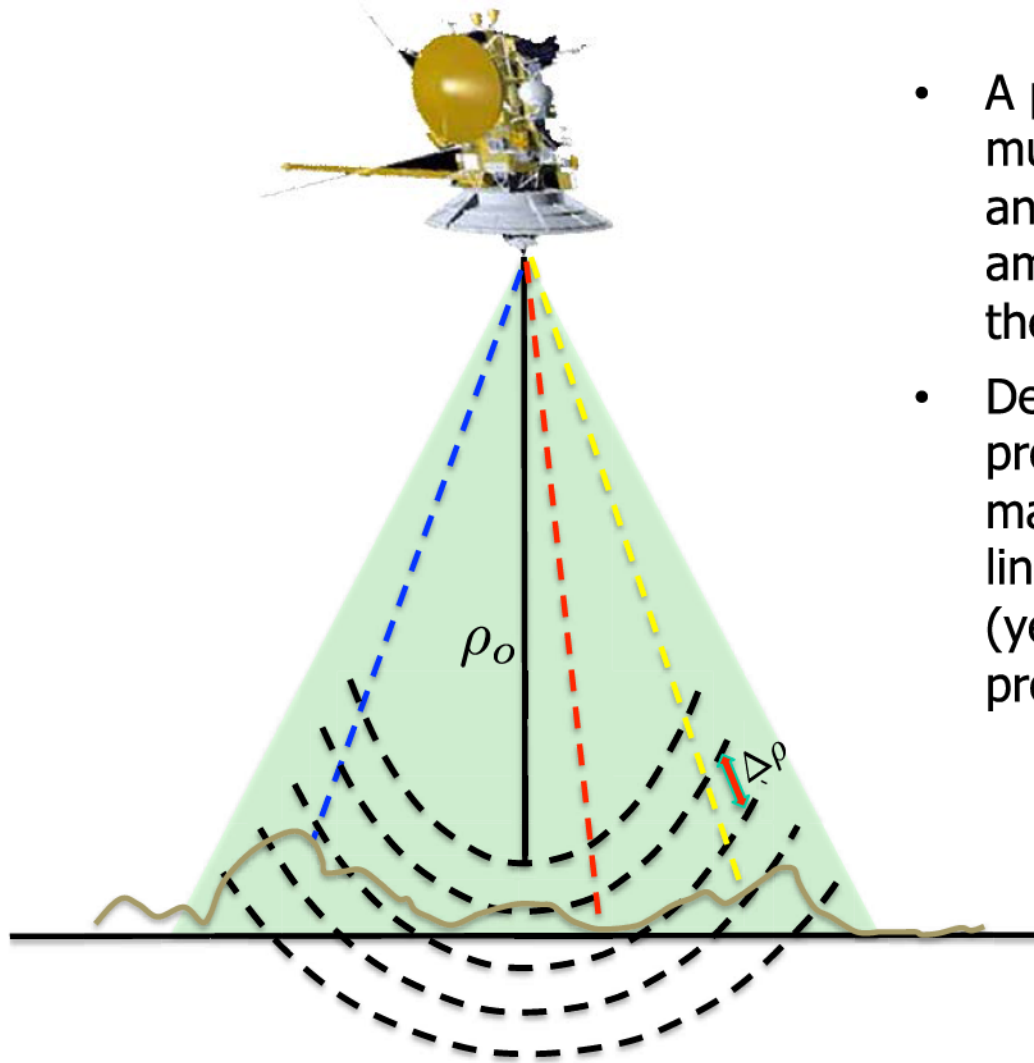
Altimeters

$$h_t = h_p - \rho$$



- Radar altimeters are downward or nadir pointing sensors that measure terrain elevation.
- Although the basic concept of altimeter operation is very simple, in practice understanding the measurement is complex due to the fact that the terrain elevation is not constant within the footprint of the antenna beam on the ground and the manner in which microwaves backscatter from the terrain.

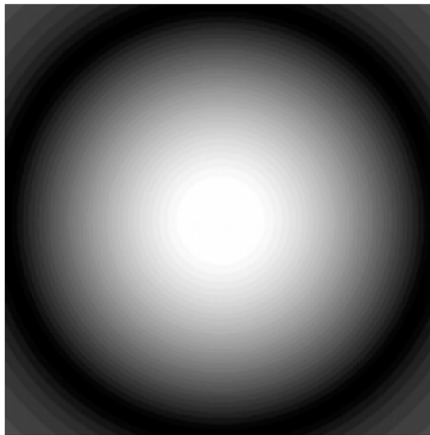
Pulse-Limited and the Echo Profile



- A pulse-limited altimeter will make multiple range measurements within an antenna footprint that is related to the amount of topographic variation called the echo profile.
- Depending on the algorithm used to process the data the reported elevation may correspond to the highest (blue line), lowest (red line) or some average (yellow line) elevation with the echo profile.

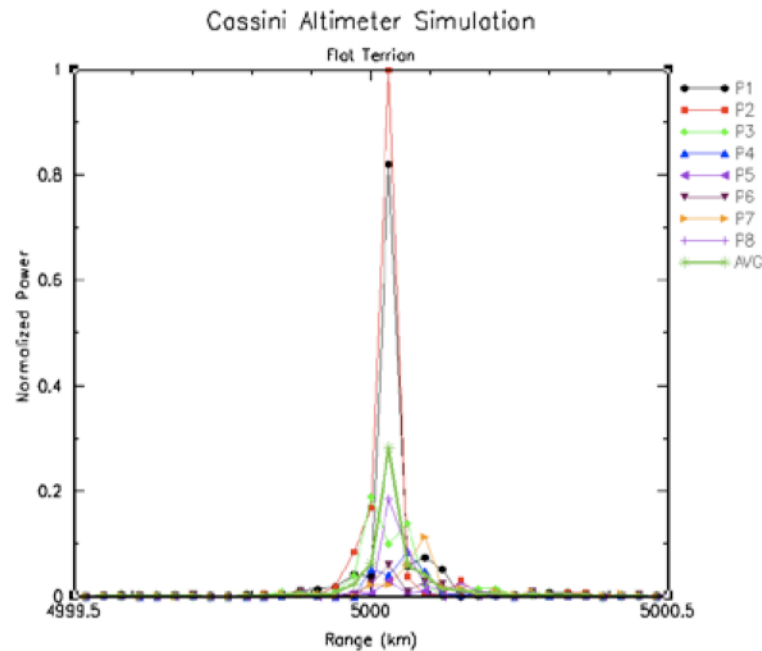
Echo Profile For a Flat Surface

Simulated Surface Reflectivity Map

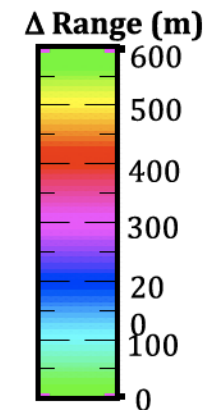
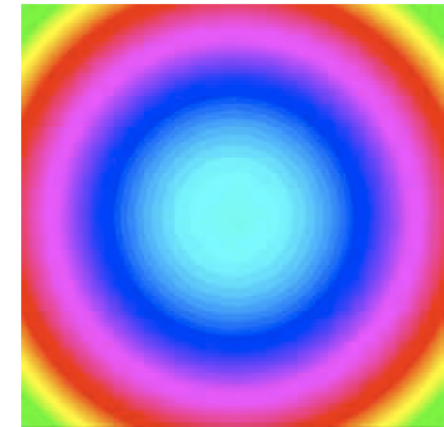


- Echo profile over simulated flat terrain
- Cassini-like altimeter at an altitude of 5000 km

Compressed Echo Profile

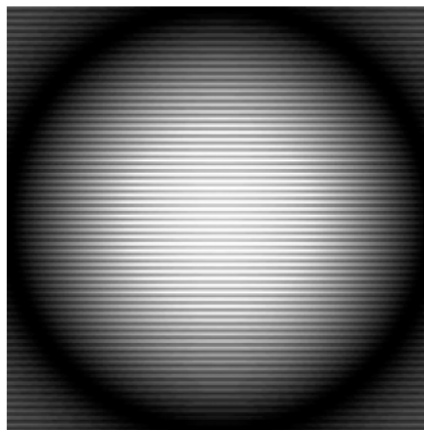


Simulated Relative Range Map



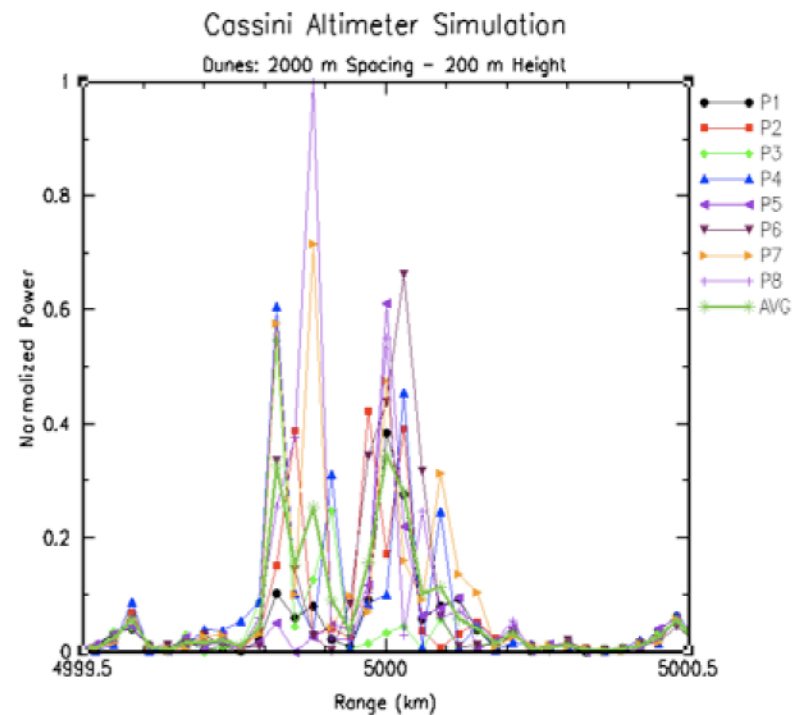
Echo Profile for Sinusoidal Hills

Simulated Surface Reflectivity Map



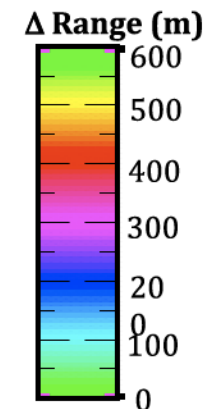
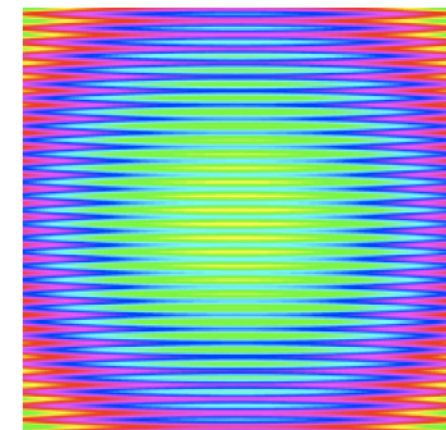
- Echo profile over simulated sinusoidal hills oriented perpendicular to the flight direction.
- Elevation Sinusoid:
 - Wavelength: 2 km
 - Amplitude: 200 m

Compressed Echo Profile

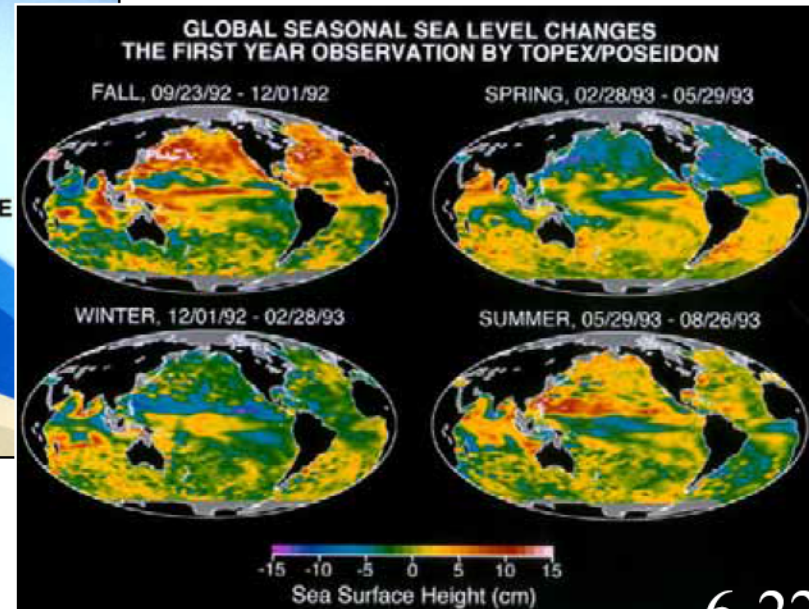
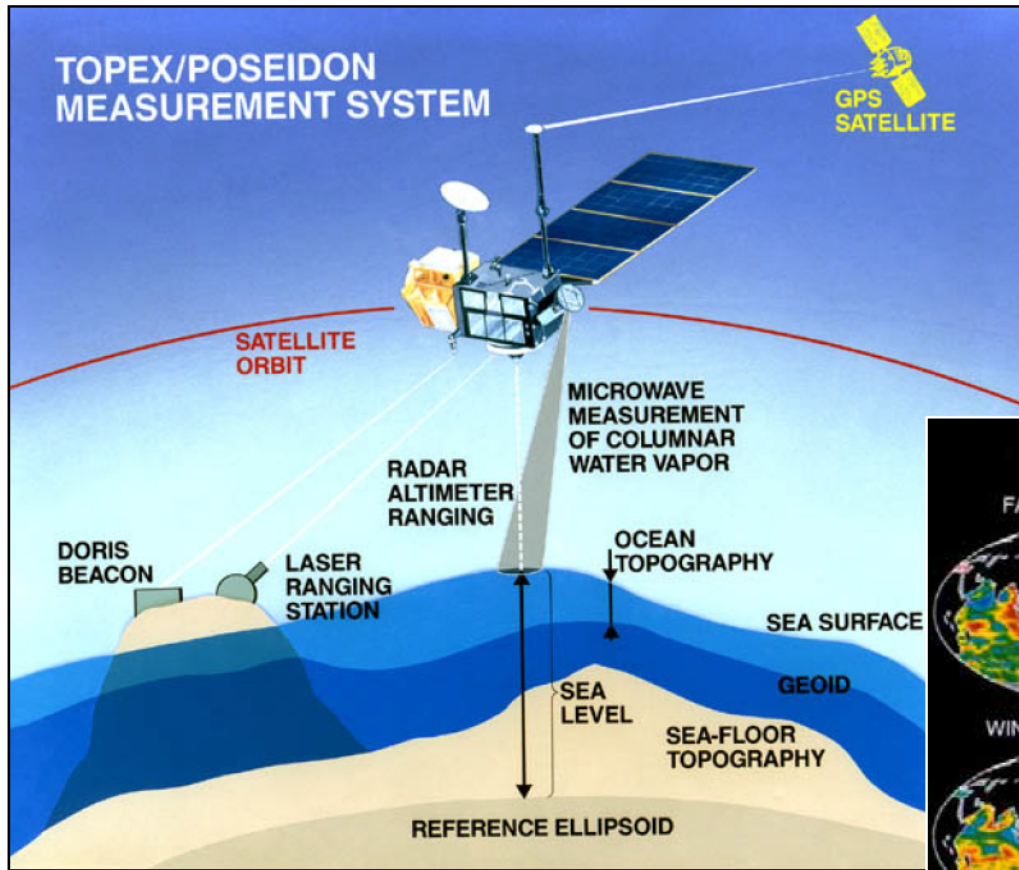


- Cassini-like altimeter at an altitude of 5000 km

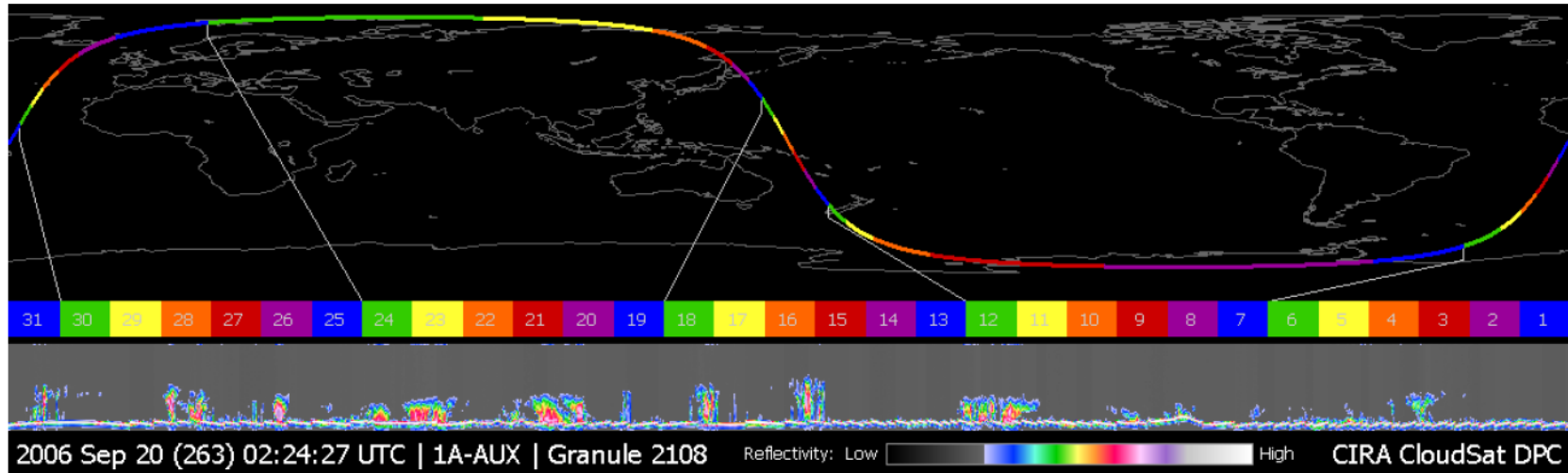
Simulated Relative Range Map



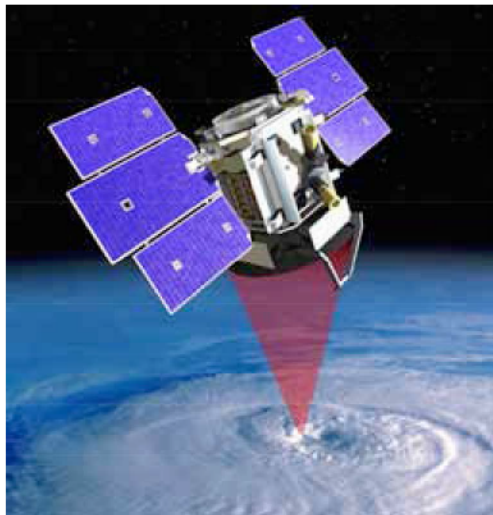
Radar Altimeters for Ocean Height Measurements



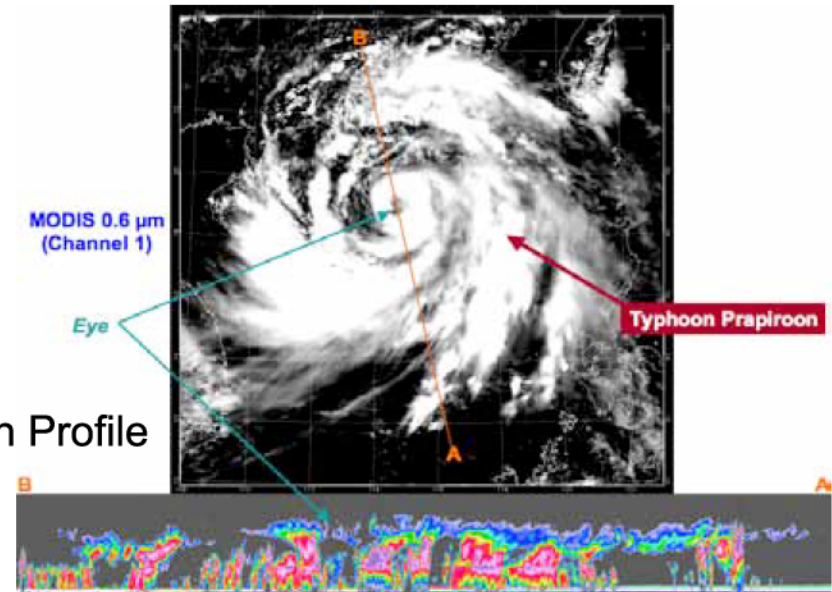
CloudSat – 94 GHz Profiling Cloud Radar



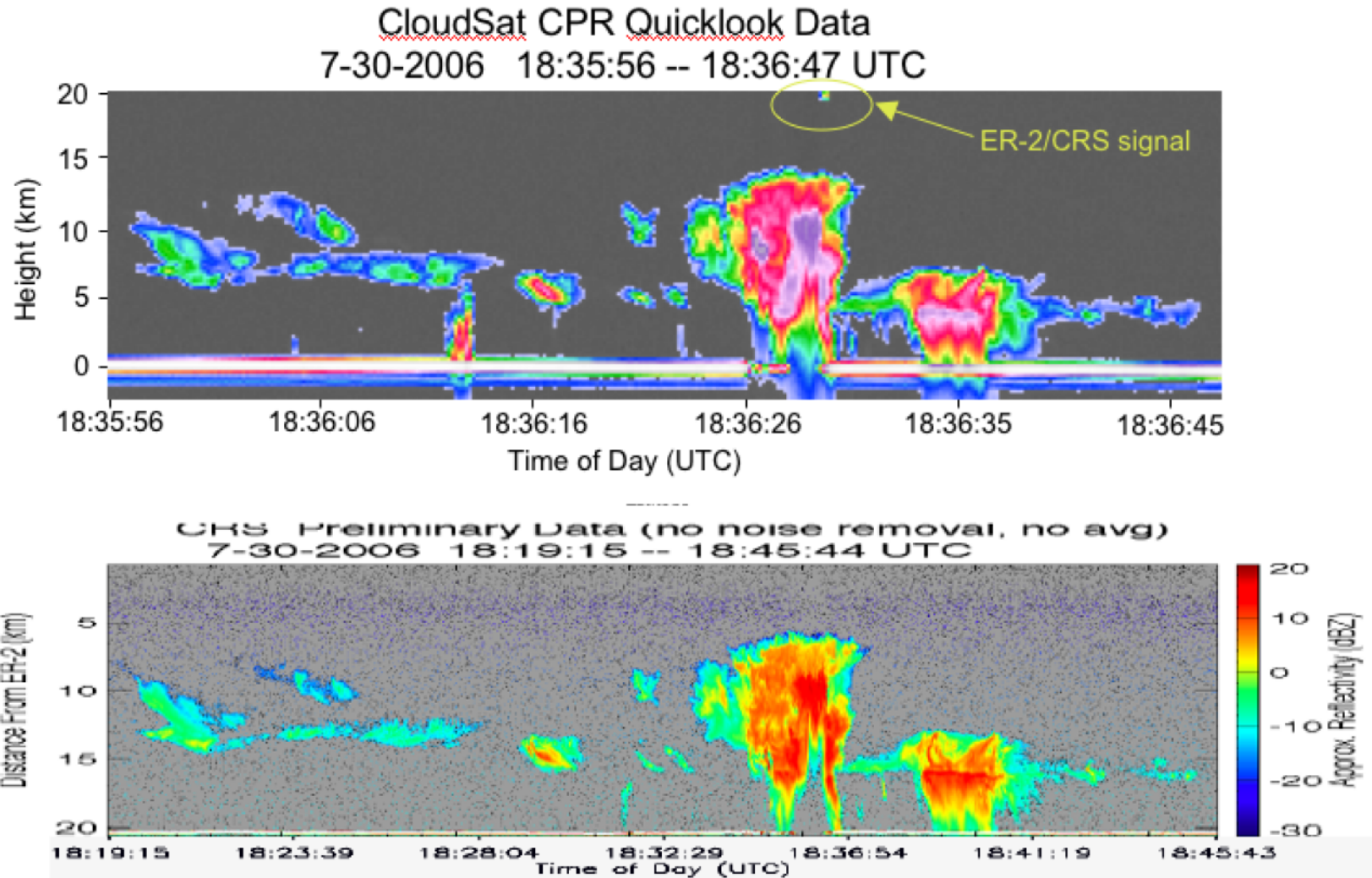
Typical Orbital Profile



Typhoon Profile



CloudSat CPR Power Returns vs Underflying ER-2 cloud radar (CRS) Reflectivity Measurements



Mars Advanced Radar for Subsurface and Ionospheric Sounding on ESA Mars Express

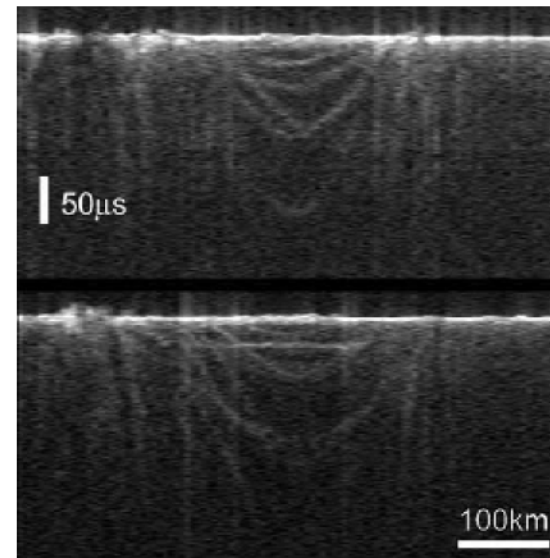


Mission/Goals

- Primary Goal: To characterize the surface and subsurface electromagnetic behavior/variation in order to elucidate the geology (Search for water, material property, stratigraphy, structure, etc) at global scales with penetration depth of up to 5 km.
- Secondary Goal: To characterize the ionosphere of Mars
- NASA OSS, “follow the water”.

Technology Areas

- Large antenna size due to low HF operation frequency)
- Complicated Matching networks due to wide relative bandwidth (0.1-5.5 MHz)
- Low frequency (HF) operation close to ionospheric plasma frequency
- Instrument calibration
- Requires specialized on-board and ground post-processing algorithms for science data calibration



Scatterometry

- Transmit a radar pulse at the surface
- Measure the backscattered energy
 - Measurement also includes thermal noise
- Subtract thermal noise from the energy measurement
 - Need to make an estimate of the thermal noise
 - Different time, different frequency, different bandwidth
 - Result is an estimate of the echo energy
- Solve the radar equation to estimate sigma-0
- Use sigma-0 measurements and the model function to infer something about the surface

$$\text{SNR} = P_T \cdot G_T(\lambda) \cdot \frac{1}{4\pi R^2} \cdot \sigma(\lambda) \cdot \frac{1}{4\pi R^2} \cdot A_R \cdot \epsilon(\lambda) \cdot \frac{1}{kTB}$$

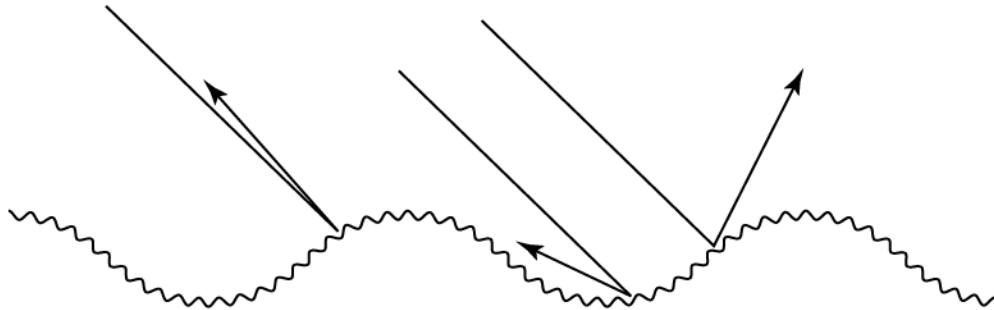
Scatterometry for Ocean Winds

Physics of ocean scattering

Bragg resonance scattering

The geometry of the ocean's surface affects its reflectivity

Wind roughens the surface of the ocean



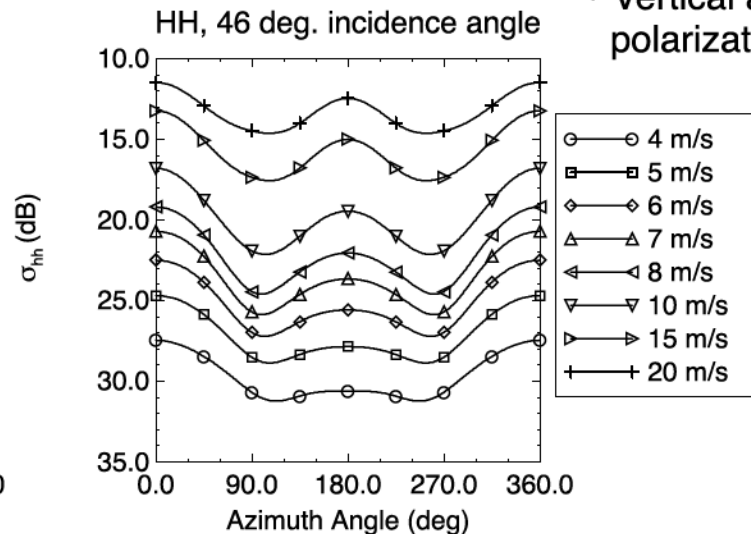
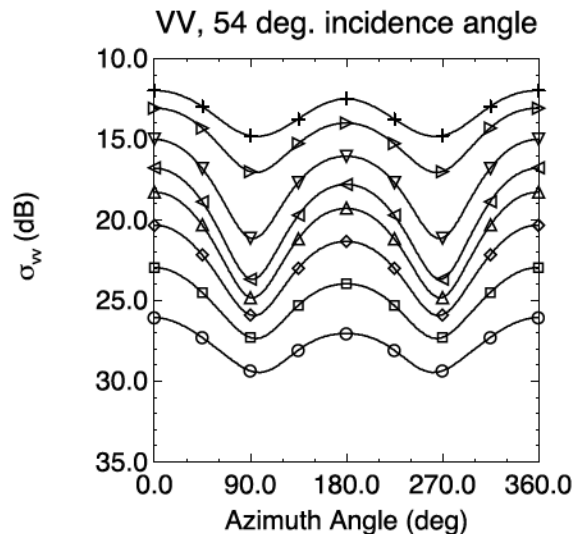
- Sigma-0 is affected by the wind speed and direction
 - Higher wind speeds roughen the surface more, increasing sigma-0
 - Wind direction aligned with the viewing vector have a larger sigma-0 than wind directions that are perpendicular
- The sigma-0 of wind-driven ocean is a function of
 - Polarization, incidence angle, wind speed, and relative wind direction
 - Other things (salinity, sea surface temperature, swells, ...)
- Sigma-0 tends to increase as incidence angles decrease

Geophysical Model Function

For a given polarization, incidence angle, and wind speed:

$$\sigma_0 = A_0 + A_1 \cos(\chi) + A_2 \cos(2\chi)$$

- Where χ is the wind direction relative to the incident radiation, and A_0 , A_1 , and A_2 are constants
- Higher order terms are used when developing the model function, but are less significant
- The model function is determined empirically by comparing sigma-0 measurements to model wind fields and/or buoy measurements

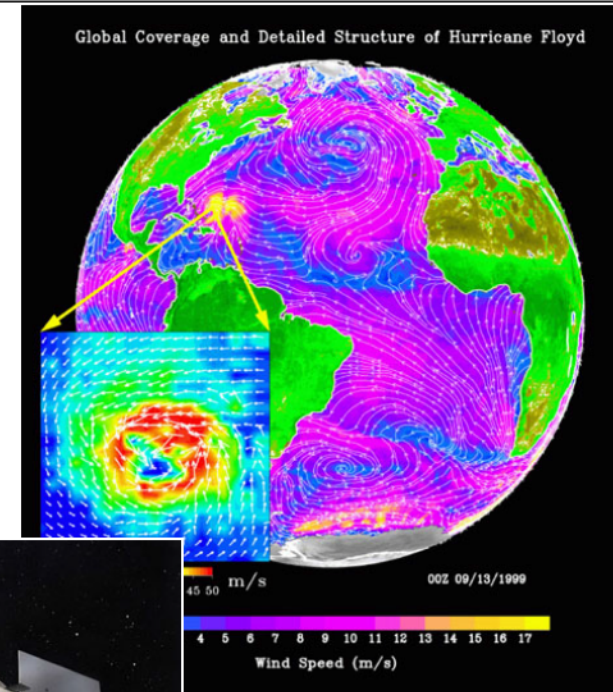


- Vertical and horizontal polarization differ

- V pol tends to have stronger backscatter than H pol
- H pol has larger upwind/downwind asymmetry
- V pol has larger upwind/crosswind asymmetry

Scatterometers for Ocean Wind

- Motivation
 - Obtain global wind vectors on a daily basis
 - Research, climatology, weather operations
 - Other applications
 - Ice edge detection, land change detection, snow cover, freeze/thaw detection, flood detection
- Scatterometers are radar instruments that measure the reflective properties of the Earth's surface
- A measure of radar reflectivity is the normalized radar cross section called sigma-0



SeaWinds



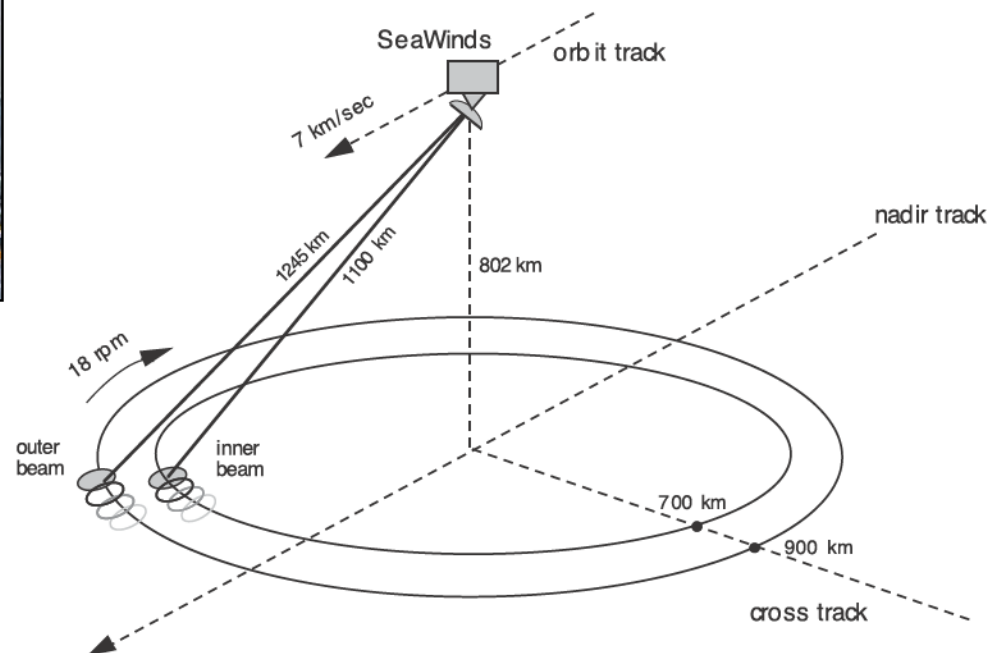
Beam geometry and polarization

Inner/Outer: H/V pol, $40^\circ/46^\circ$ look angle,
 $46^\circ/54^\circ$ incidence angle

RF: 13.402 GHz, Ku band, 185 Hz PRF

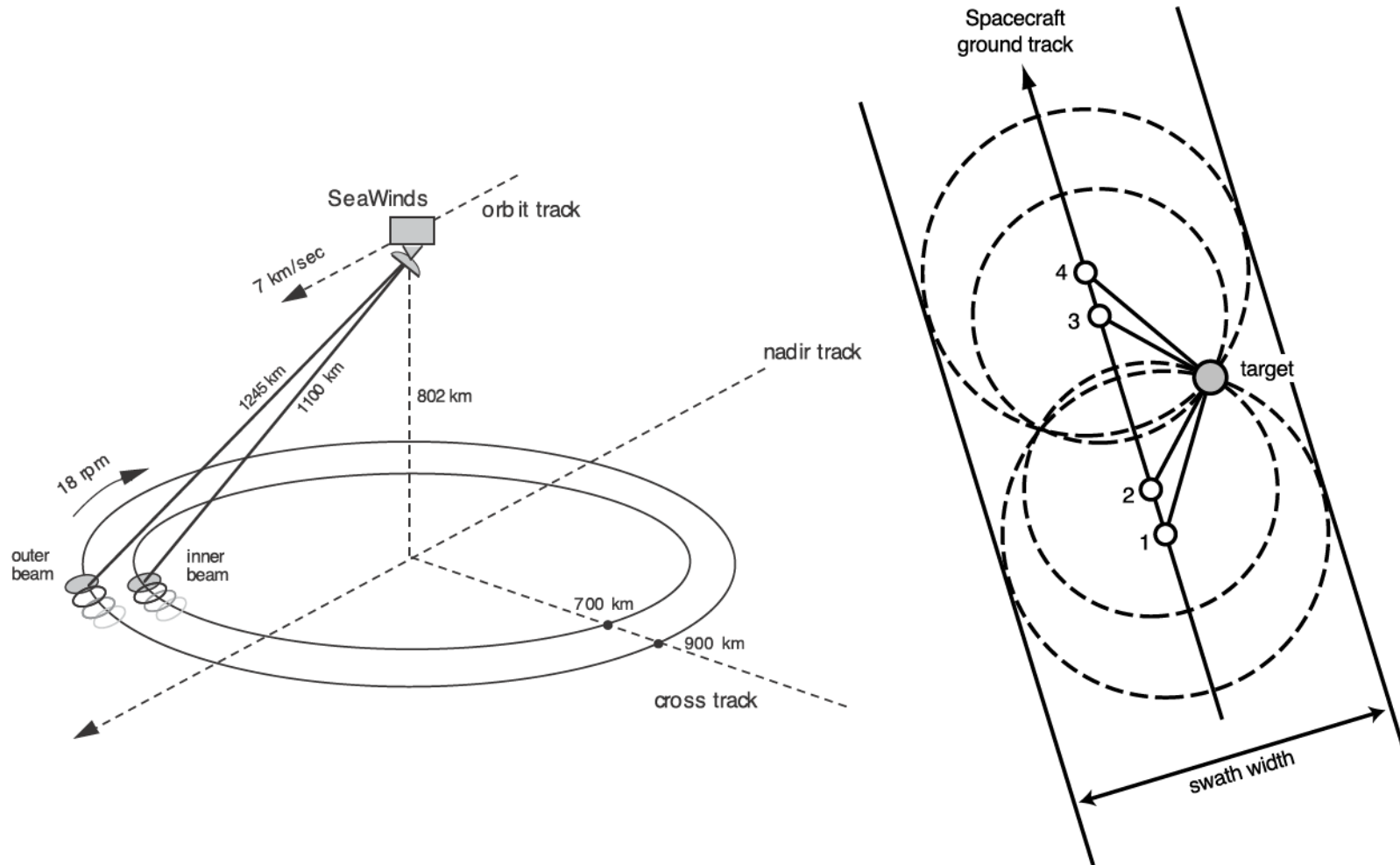
Swath width

1400/1800 km for inner/outer beam

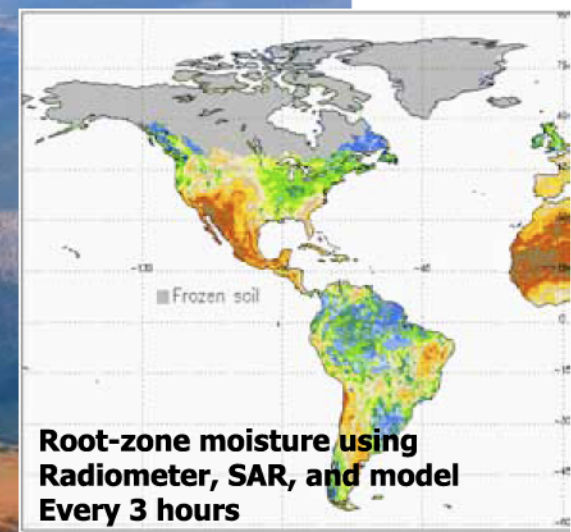
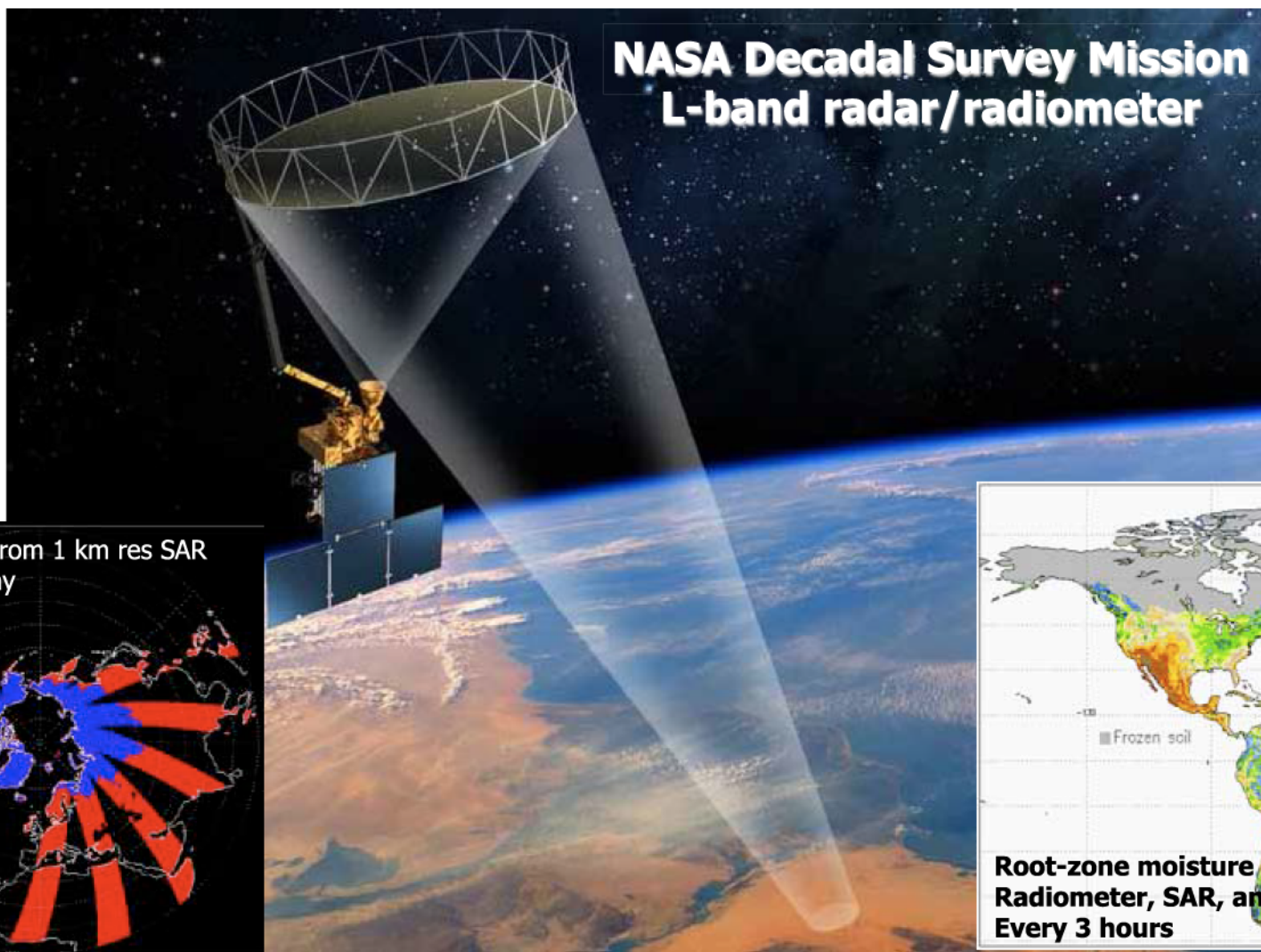


90% daily coverage

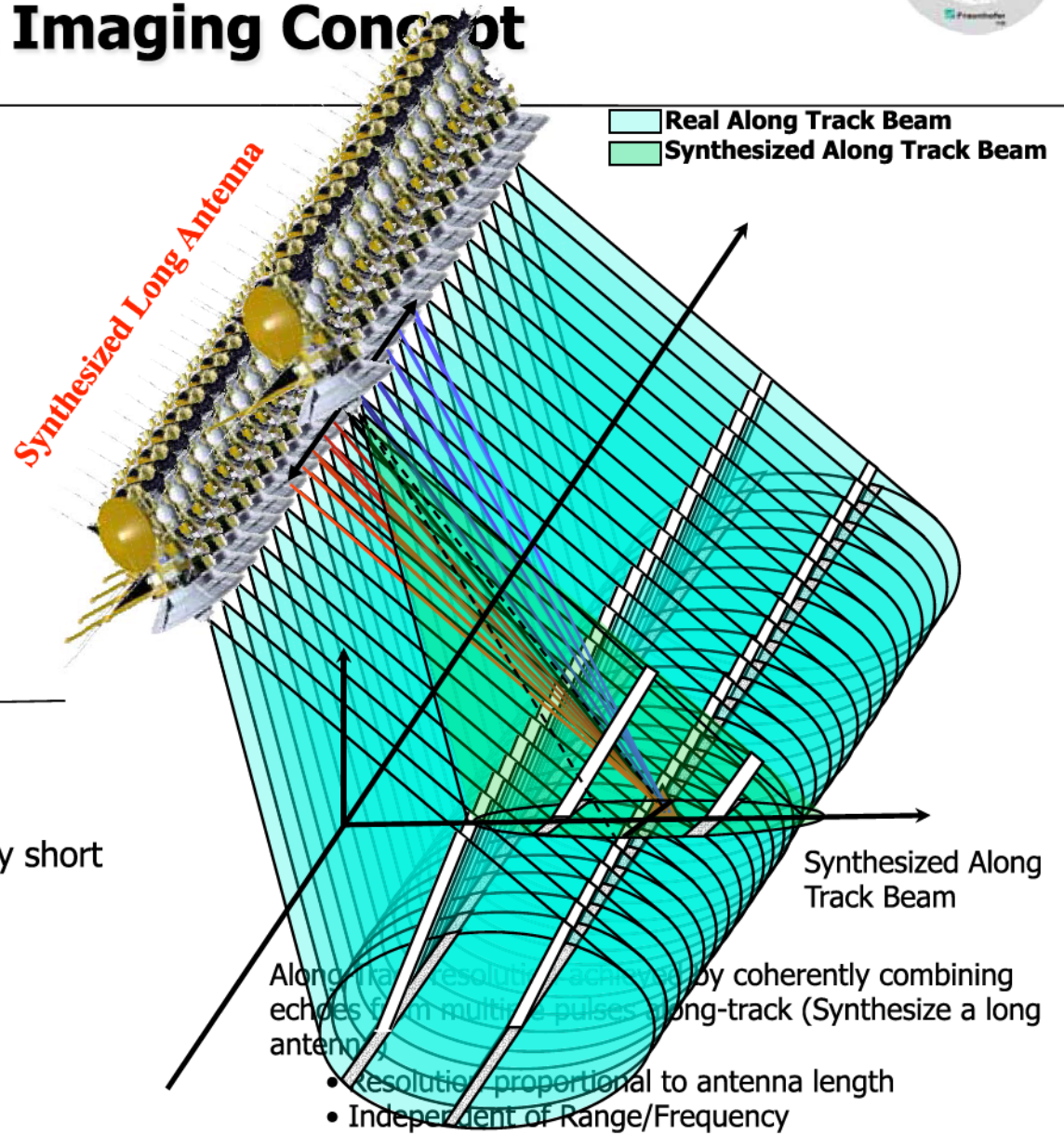
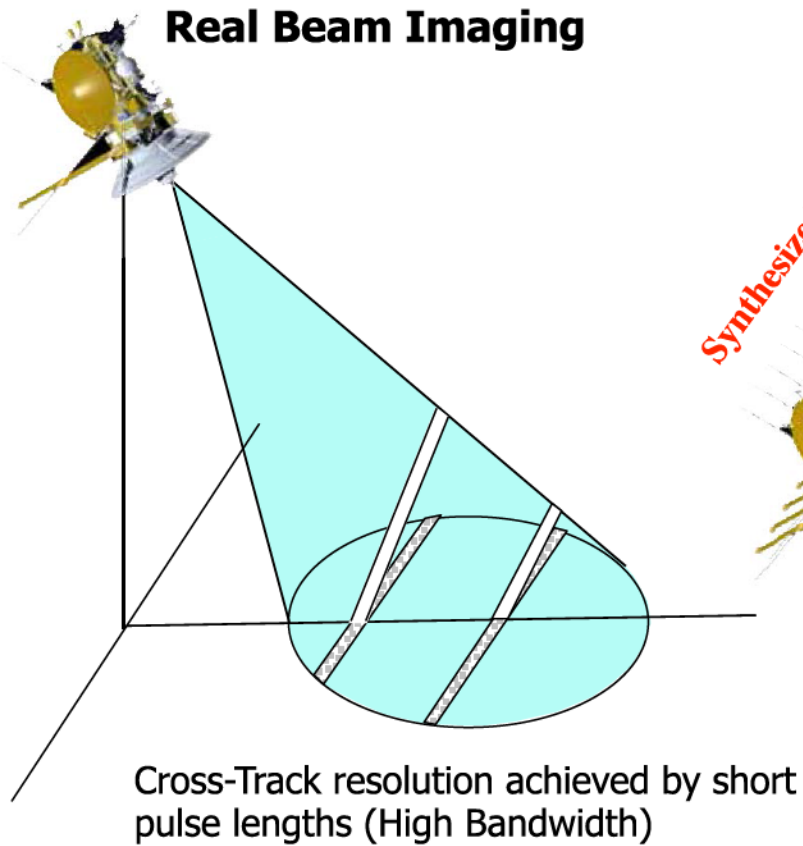
Wind Vector Cell Geometry



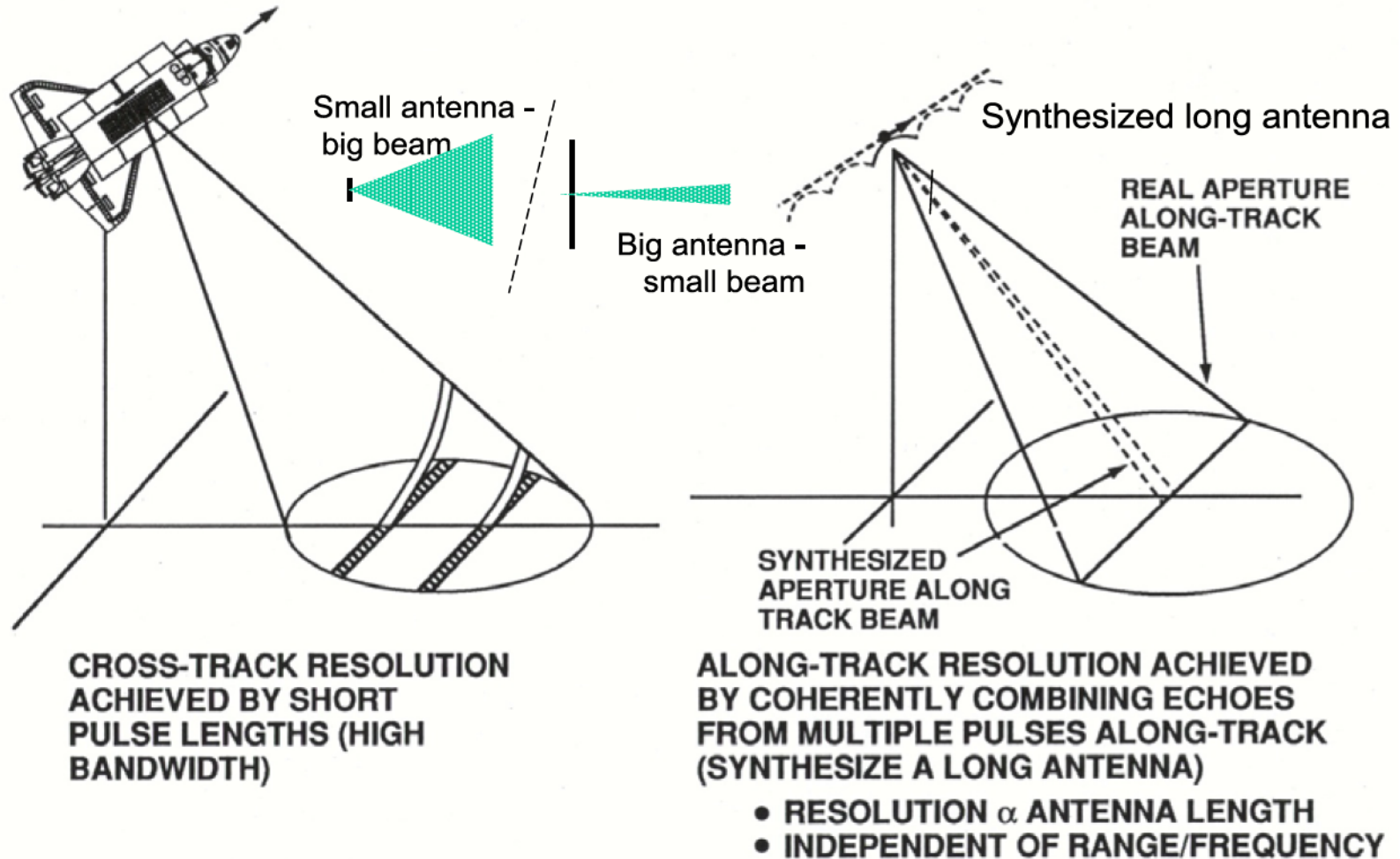
Soil Moisture Active/Passive (SMAP)



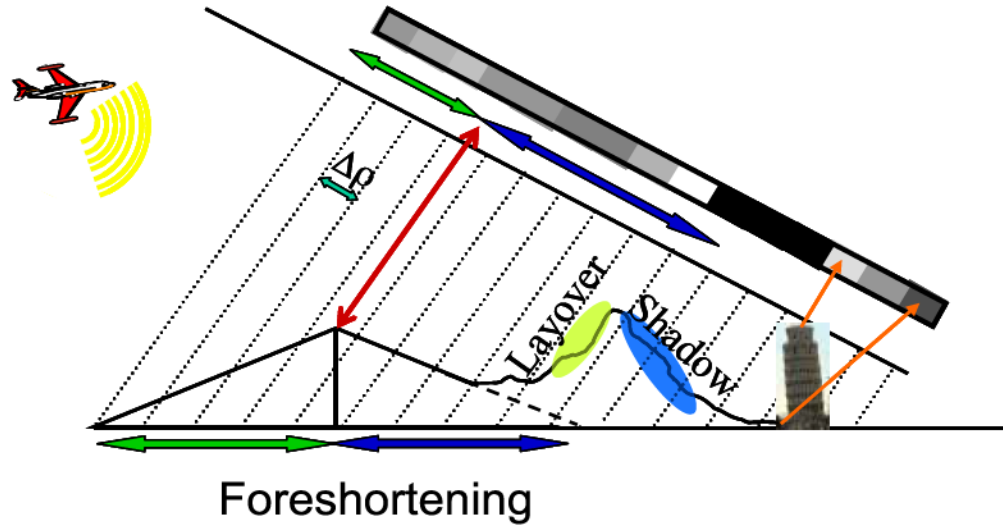
SAR Imaging Concept



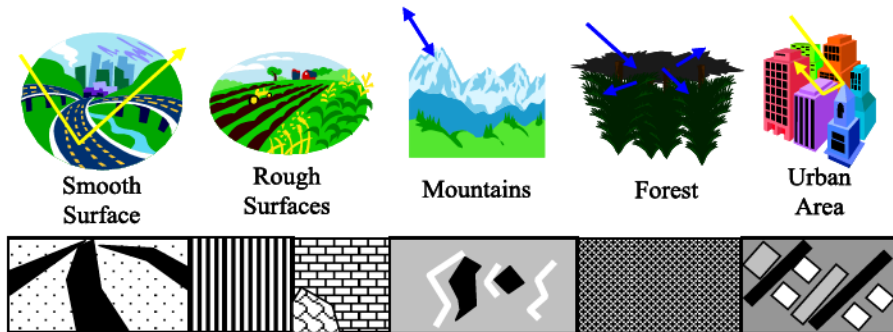
Imaging Radar



Radar Imaging Properties



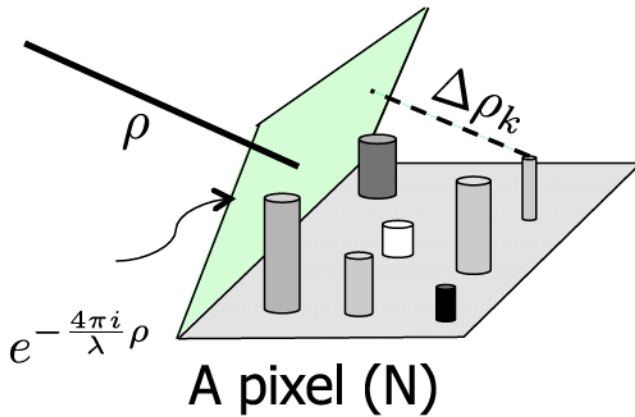
- Radar images are distorted relative to a planimetric view
- Slopes facing toward or away from the radar appear foreshortened
- Steep slopes are collapsed into a single range cell called layover and areas occulted by other areas are said to be shadowed



- Radar is primarily sensitive to the structure of objects being imaged whereas optical images are primarily sensitive to chemistry
- The scale of objects relative to the radar wavelength determines how smooth an object appears to the radar and how bright or dark it is in the imagery

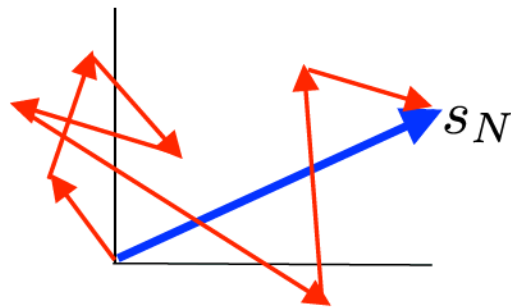
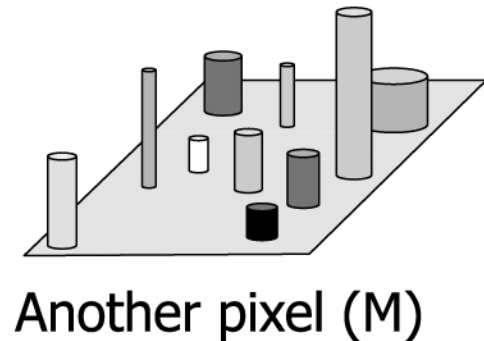
SAR Imagery and Speckle

The total signal return s_x from a resolution cell X is the coherent sum of the individual contributions of each scatterer within it. For natural surfaces, scatterers are generally modelable as randomly distributed in space.

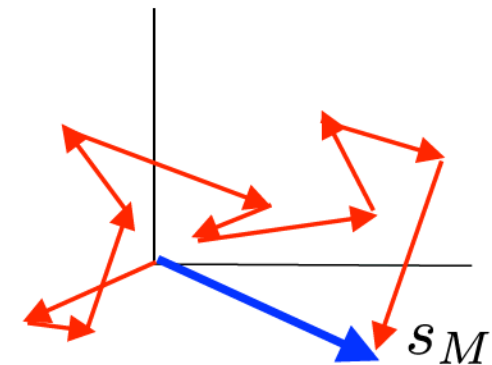


Number and arrangement of scattering elements within resolution cell varies from pixel to pixel.

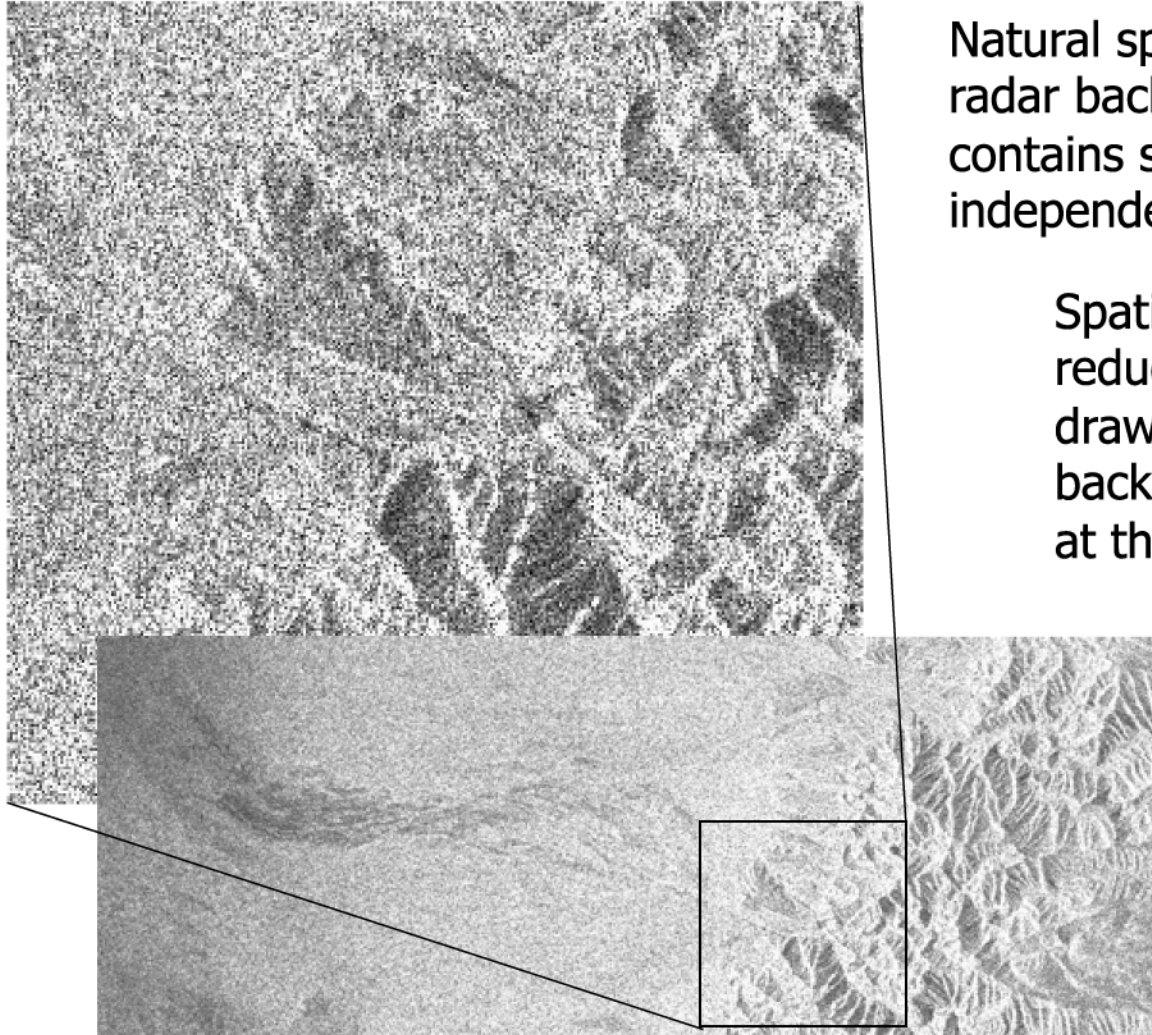
Returned signal is a coherent combination of the returns from the scattering elements.



$$s = A \underbrace{e^{-\frac{4\pi i}{\lambda} \rho}}_{\text{Range Phase}} \underbrace{\sum_{k=1}^N a_k e^{-\frac{4\pi i}{\lambda} \Delta \rho_k}}_{\text{Scatterer Contribution}}$$



Speckle and Radiometric Accuracy



Natural speckle masks intrinsic radar backscatter which contains surface information, independent of SNR!

Spatial averaging (looks) reduces the speckle and draws out the natural backscatter reflectivity, at the cost of resolution

$$\bar{s}_k = \sqrt{\frac{1}{2L} \sum_{i=k-L}^{k+L-1} s_i^2}$$

Spatial Averaging or Looks

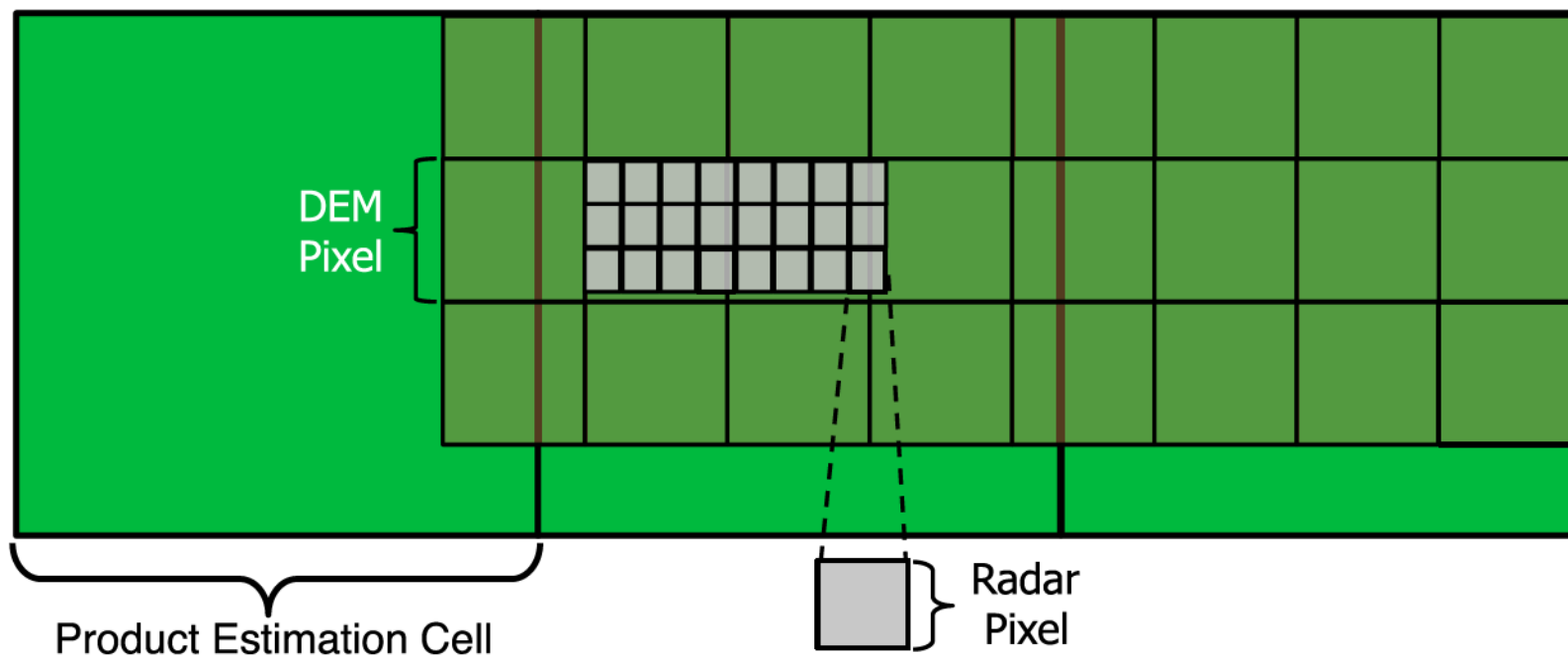
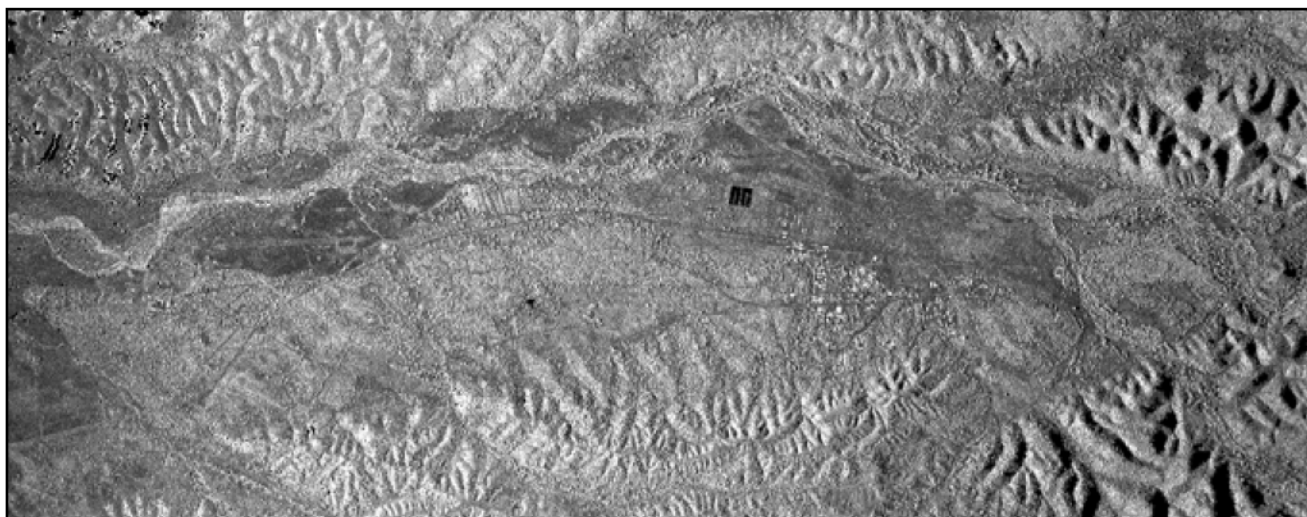
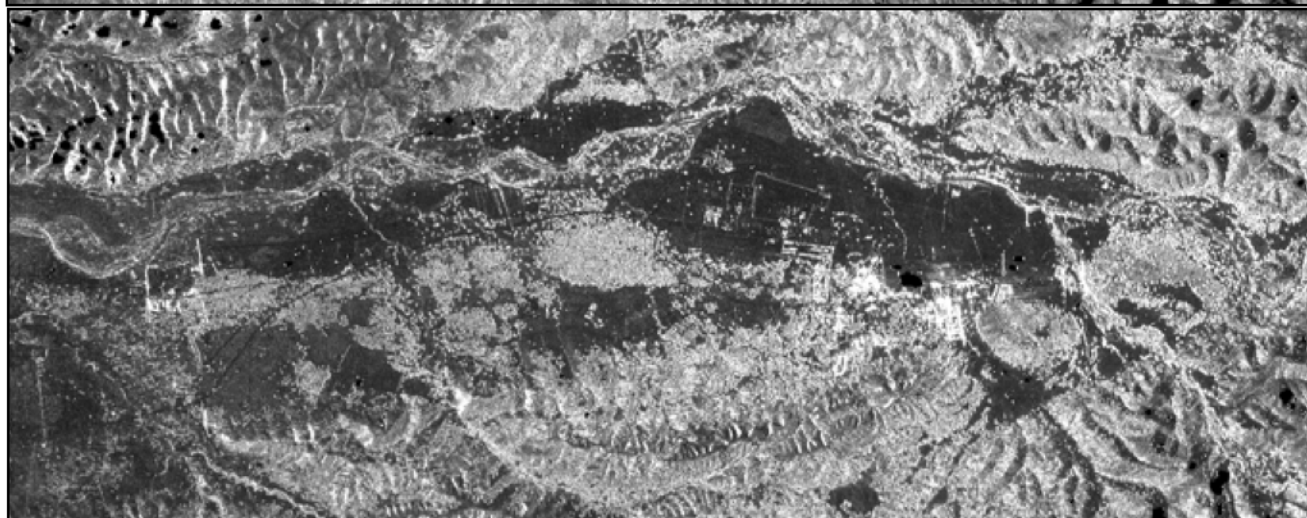


Image Frequency Comparison



X-band
3 cm



P-band
85 cm

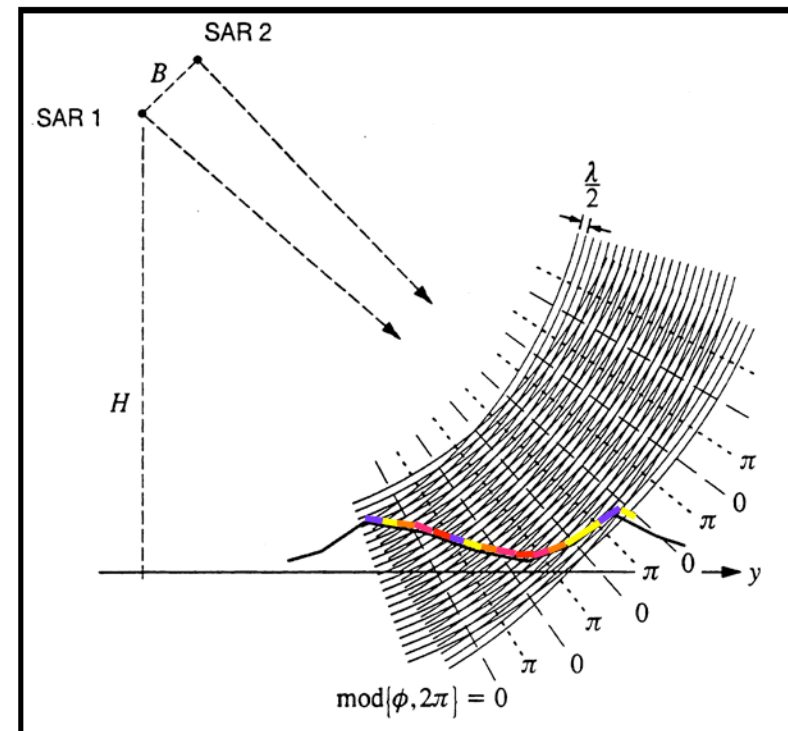
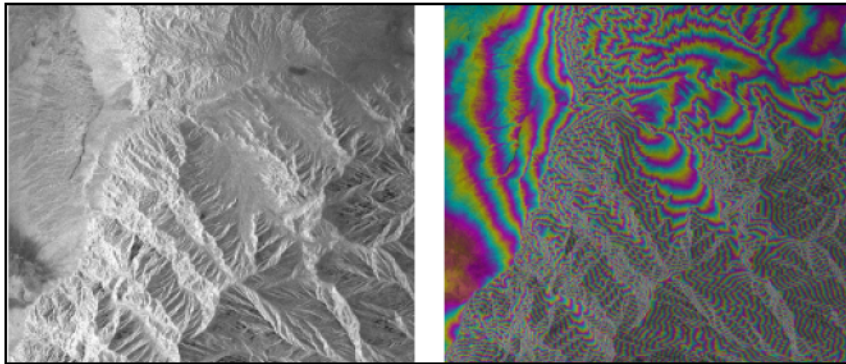
Visible (Upper) and Radar (Lower)



Nile in Sudan Showing Ancient Nile Course

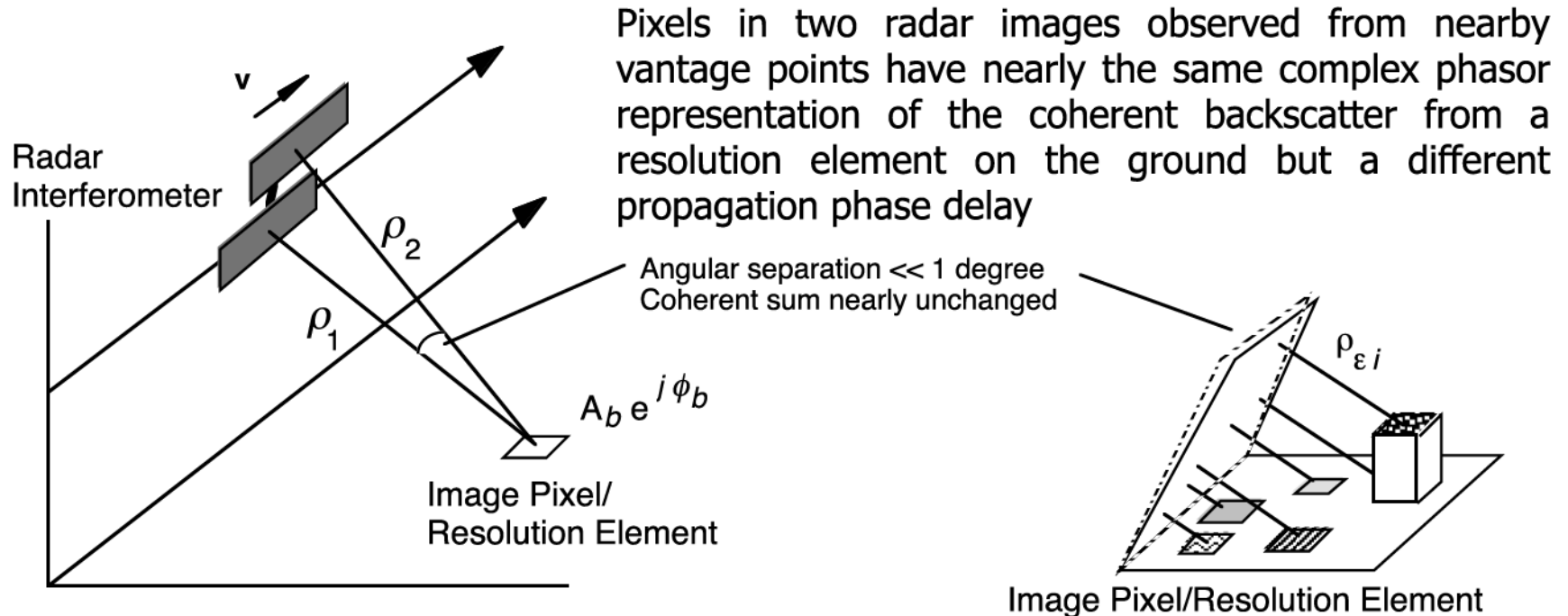
Radar Interferometry

- Radar has a coherent source much like a laser
- The two radar (SAR) antennas act as coherent point sources
- When imaging a surface, the phase fronts from the two sources interfere
- The surface topography slices the interference pattern



- The measured phase differences record the topographic information

Interferometric Phase Characteristics

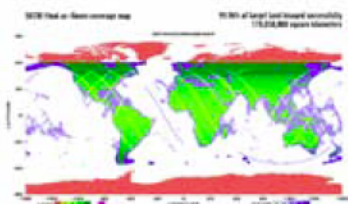


$$s_1 = A_b e^{j\phi_b} e^{-j\frac{4\pi}{\lambda}\rho_1} \quad s_2 = A_b e^{j\phi_b} e^{-j\frac{4\pi}{\lambda}\rho_2}$$

$$s_{int} = s_1 s_2^* = A_b e^{j\phi_b} e^{-i\frac{4\pi}{\lambda}\rho_1} A_b e^{-i\phi_b} e^{i\frac{4\pi}{\lambda}\rho_2} = A_b^2 e^{i\frac{4\pi}{\lambda}(\rho_2 - \rho_1)}$$

Coherent backscatter term that is random from cell-to-cell cancels leaving phase that depends on differential path length!

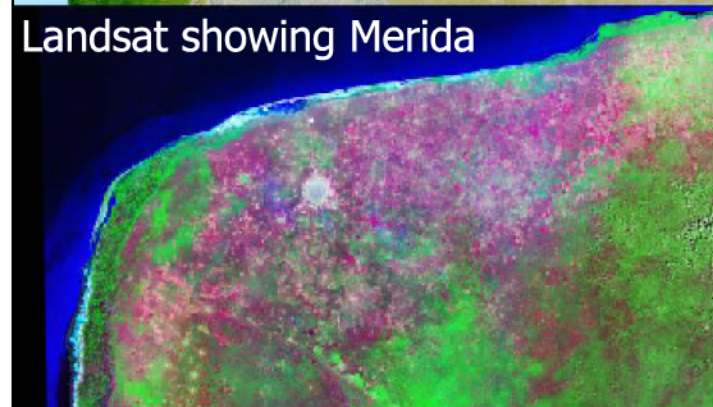
Shuttle Radar Topography Mission (SRTM)



SRTM image of Yucatan showing Chicxulub Crater, site of K-T extinction impact.



Landsat showing Merida

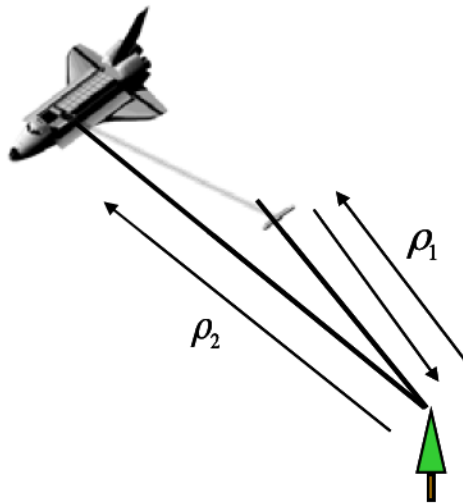


3-dimensional SRTM view of Los Angeles (with Landsat data) showing San Andreas fault

Data Collection Approaches

Single Pass

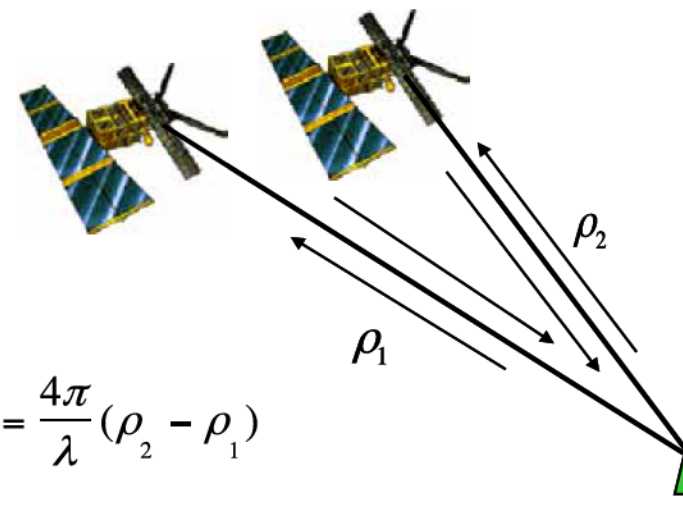
- Interferometric radar data can be collected in a single pass interferometry (SPI) mode where both antennas are located on the same platform. One antenna transmits and both antennas receive the returned echoes



$$\phi = \frac{2\pi}{\lambda}(\rho_2 - \rho_1)$$

Repeat Pass

- In the repeat pass mode (RPI) two spatially close radar observations of the same scene are made separated in time. The time interval may range from seconds to years

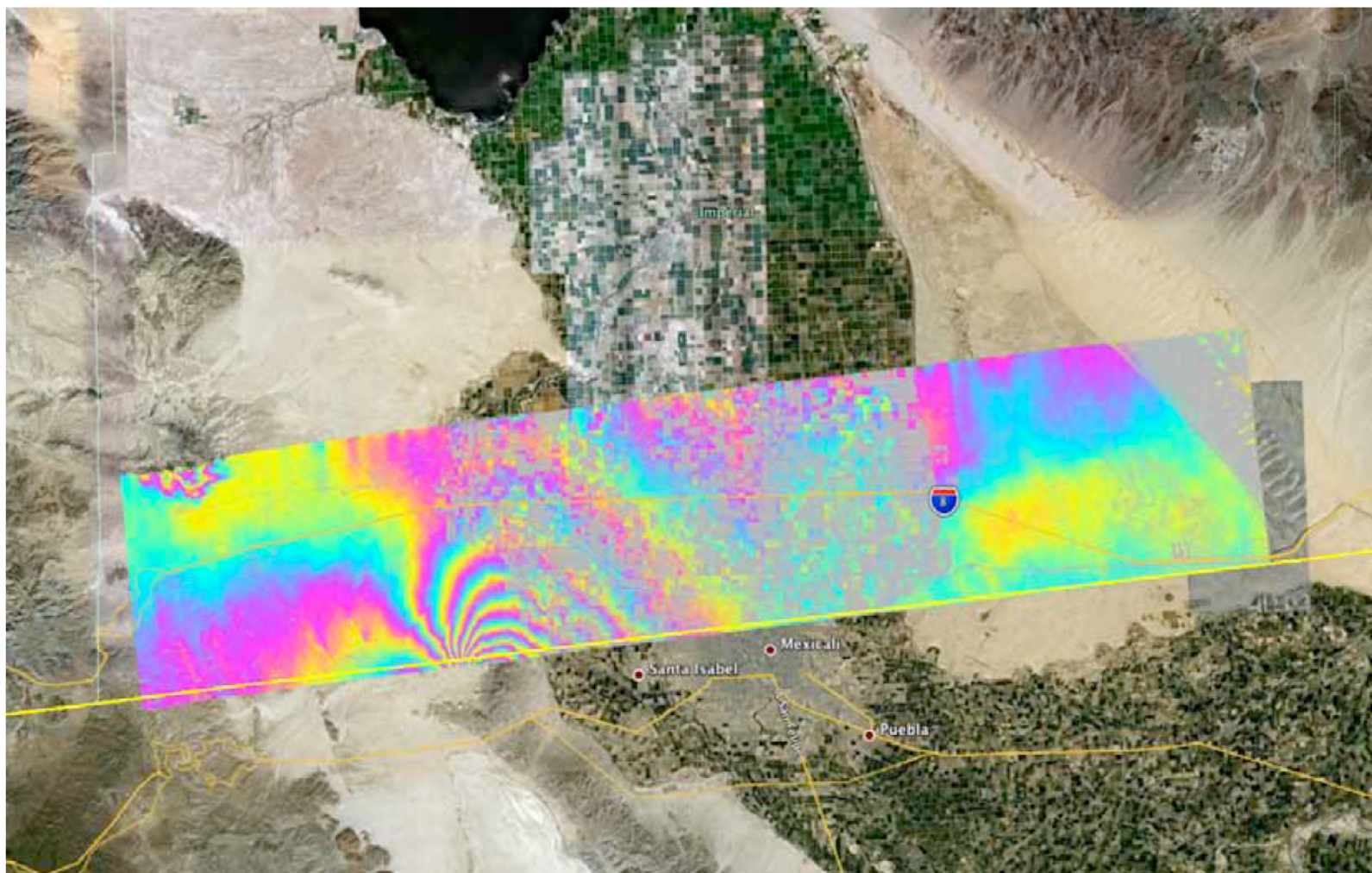


$$\phi = \frac{4\pi}{\lambda}(\rho_2 - \rho_1)$$

- Temporal decorrelation — scene changes between observations
- Propagation delay variations — changes in troposphere or ionosphere between observations

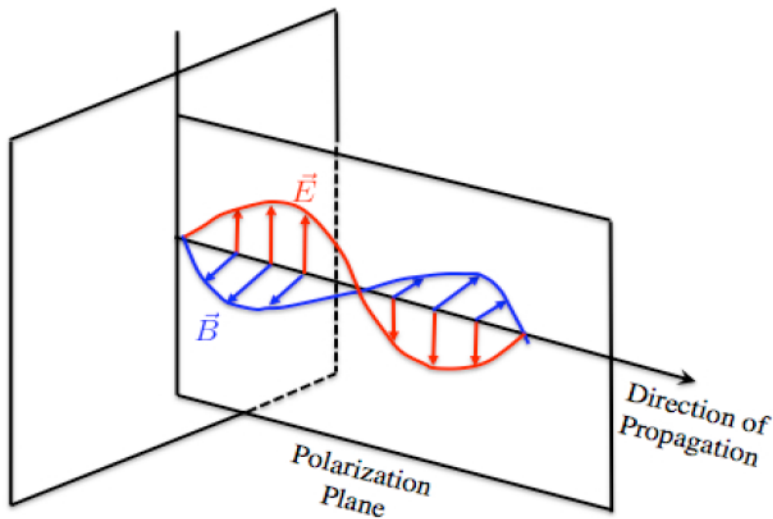
April 4, 2010 M 7.2 Baja California Earthquake

Airborne repeat-pass InSAR for geodetic imaging



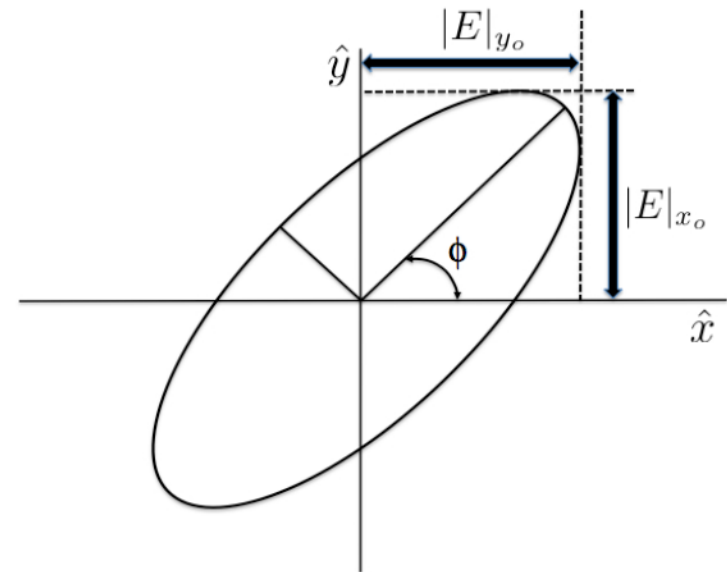
Polarization

- The electric and magnetic fields comprising an electromagnetic wave are vector fields. The direction of the electric and magnetic field lies in the plane perpendicular to the direction of propagation and defines the polarization of the wave.
 - Polarization may be linear, circular or elliptical depending on the trace of the electric field vector in a plane perpendicular to the direction of propagation.



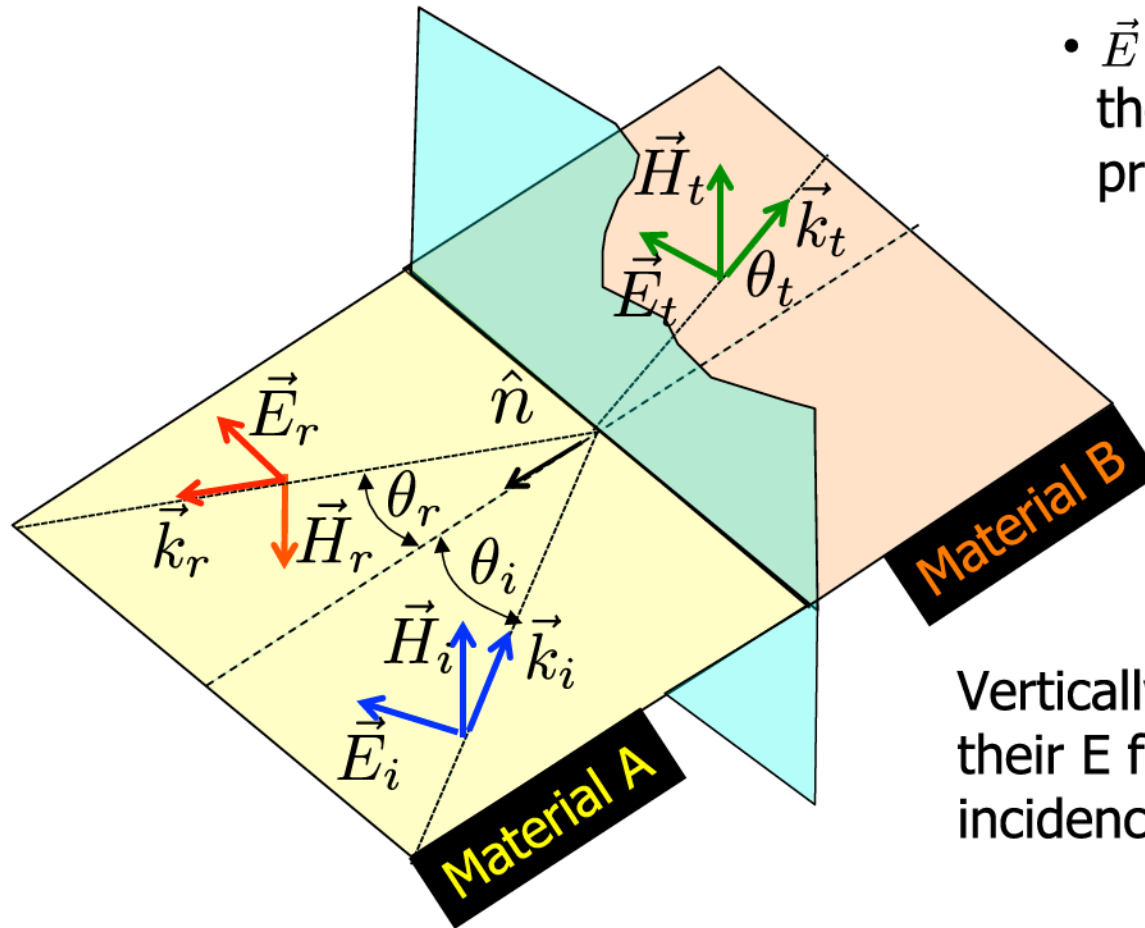
Linearly polarized wave

Locus of E in plane of E and B



Polarization and Incidence Planes

Vertical Polarization



- $\vec{E} \times \vec{H}$ always points in the direction of propagation

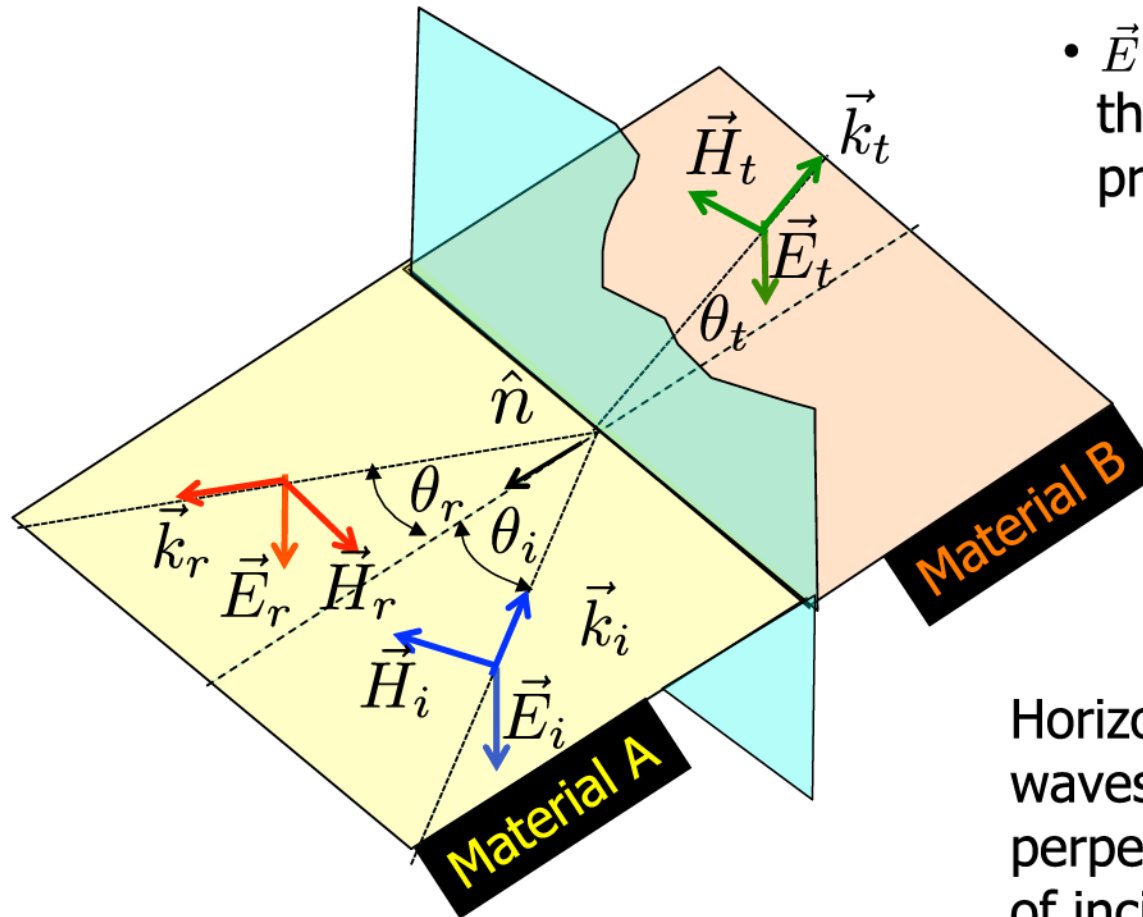
$$\hat{k} = \frac{\vec{E} \times \vec{H}}{|\vec{E} \times \vec{H}|}$$

Vertically polarized waves have their E field in the plane of incidence.

Plane of incidence defined by \hat{n} and \vec{k}_i
 Plane of polarization defined by \vec{E}_i and \vec{k}_i

Polarization and Incidence Planes

Horizontal Polarization



- $\vec{E} \times \vec{H}$ always points in the direction of propagation

$$\hat{k} = \frac{\vec{E} \times \vec{H}}{|\vec{E} \times \vec{H}|}$$

Horizontally polarized waves have their E field perpendicular to the plane of incidence.

Plane of incidence defined by \hat{n} and \vec{k}_i
 Plane of polarization defined by \vec{E}_i and \vec{k}_i



Scattering From a Flat Plate – Boundary Conditions

- It is possible to derive the magnitude and phase of the reflected and transmitted phase at an interface from the fact that the tangential components of the E and H fields must be continuous across the interface.
- Continuity implies
 - The incident, reflected and transmitted fields are identical functions of time
 - The incident, reflected and transmitted fields are identical function of position on the interface
- The first condition means all three waves have the SAME frequency.
- The second condition implies
 - The angle of incidence equals the angle of reflection
 - That all three waves are co-planar
 - Finally, the incident and transmitted angles satisfy Snell's law

$$\frac{\sin \theta_t}{\sin \theta_i} = \frac{n_A}{n_B} = \frac{\sqrt{\epsilon_A \mu_A}}{\sqrt{\epsilon_B \mu_B}}$$

ϵ = Relative permittivity
 μ = Relative permeability
 $\tilde{\epsilon} = \text{dielectric constant} = n^2$

Fresnel Reflection Coefficients

From the continuity of the tangential fields the reflection coefficients (ratio of reflected amplitude to incident amplitude) and transmission coefficients (ratio of transmitted amplitude to incident amplitude) are given by:

Horizontal Polarization

$$R = \frac{n_B \cos \theta_i - n_A \cos \theta_t}{n_A \cos \theta_t + n_B \cos \theta_i}$$

$$T = \frac{2n_A \cos \theta_i}{n_A \cos \theta_t + n_B \cos \theta_i}$$

Vertical Polarization

$$R = \frac{n_A \cos \theta_i - n_B \cos \theta_t}{n_A \cos \theta_i + n_B \cos \theta_t}$$

$$T = \frac{2n_A \cos \theta_i}{n_A \cos \theta_i + n_B \cos \theta_t}$$

Note that these are complex quantities, having both magnitude and phase.

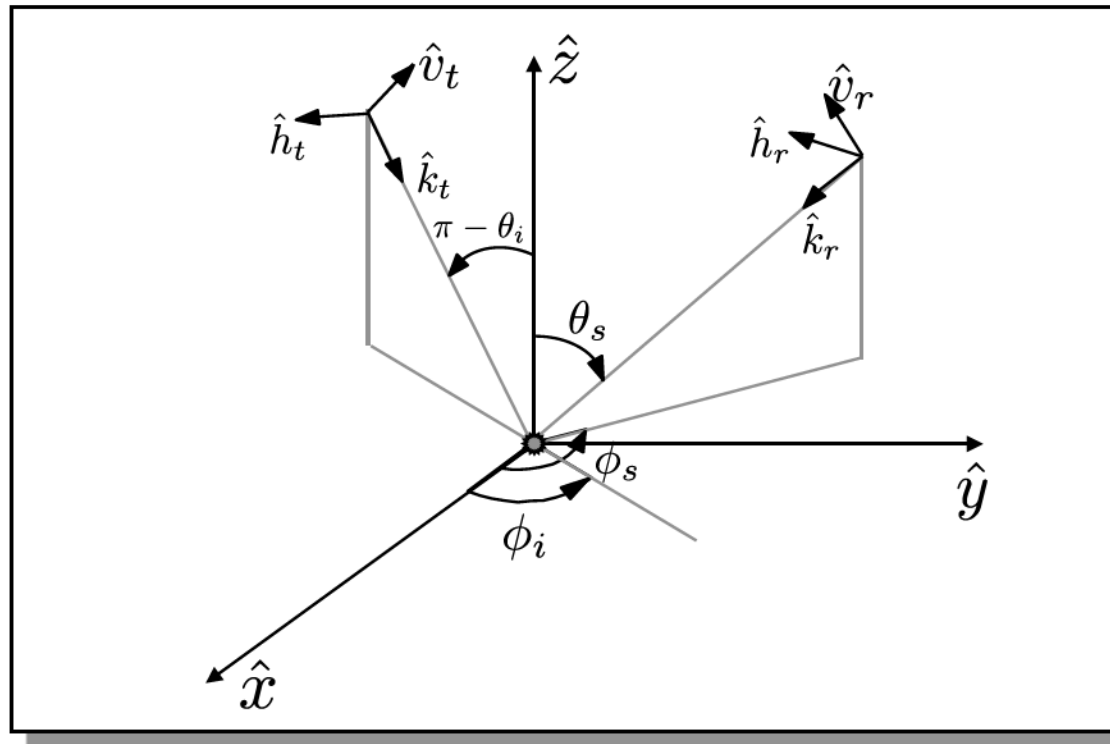
Brewster Angle

- For vertically polarized waves (E field in the plane of incidence) there is angle at which there is no reflected signal. This angle is called the *Brewster angle*.
- For horizontal waves there is only the trivial solution $n_A = n_B$.

$$\begin{aligned}
 n_A \cos \theta_i &= n_B \cos \theta_t && \text{Numerator of } R_V \\
 n_A^2 \cos^2 \theta_i &= n_B^2 \left(1 - \left(\frac{n_B}{n_A} \right)^2 \sin^2 \theta_i \right) \\
 &\cdot \\
 &\cdot \\
 &\cdot \\
 \tan^2 \theta_i &= \frac{n_A^2 - n_B^2}{n_A^2} \frac{n_B^2}{n_A^2 - n_B^2} = \frac{n_B^2}{n_A^2} \\
 \tan \theta_i &= \frac{n_B}{n_A} && \text{Brewster Angle condition}
 \end{aligned}$$

Coordinate Systems

Matrices and vectors are measured using the ***backscatter alignment*** coordinate system. This system is preferred when calculating radar-cross sections, and is used when measuring them:



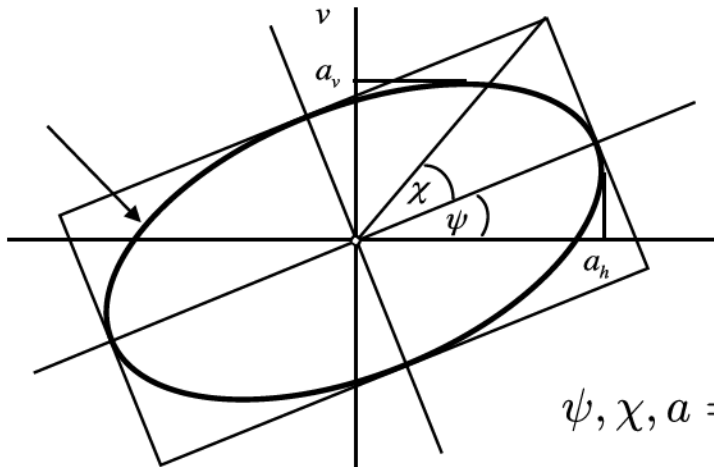
Polarimetric Representations

Polarization Vector

$$\vec{p} = \begin{bmatrix} a_h \\ a_v \end{bmatrix}$$

Polarization Ellipse

- Various forms of the polarization ellipse are normally characterized by two values:
 - The tilt which gives the orientation of the ellipse (ψ)
 - The ellipticity angle (χ) is a measure of the shape of the ellipse



$$\psi, \chi, a = |a_h|^2 + |a_v|^2$$

Stokes Vector

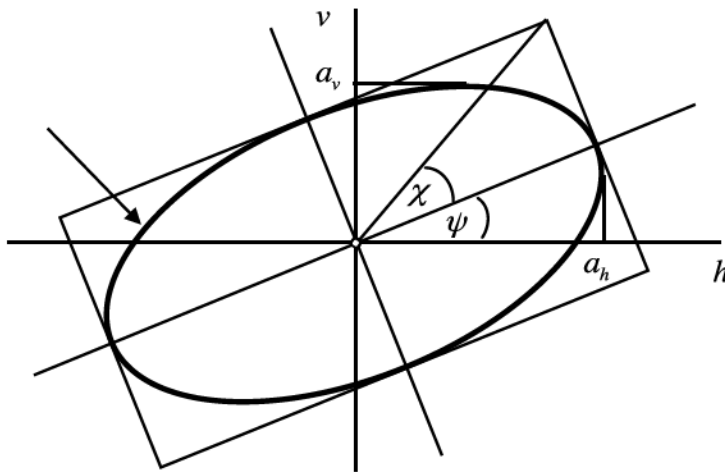
- Stokes parameters are the same independent of polarization basis used to compute them.

$$\vec{S} = \begin{bmatrix} S_0 \\ S_1 \\ S_2 \\ S_3 \end{bmatrix} = \begin{bmatrix} |a_h|^2 + |a_v|^2 \\ |a_h|^2 - |a_v|^2 \\ 2\mathcal{R}(a_h a_v^*) \\ 2\mathcal{I}(a_h a_v^*) \end{bmatrix}$$

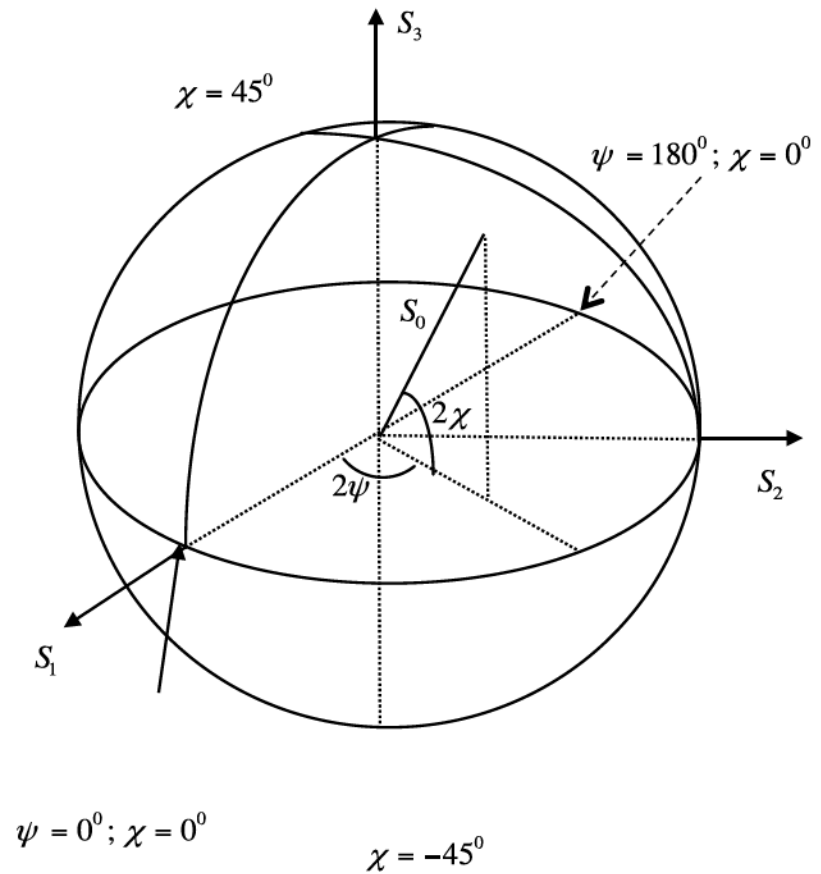
$$= \begin{bmatrix} |a_h|^2 + |a_v|^2 \\ S_0 \cos 2\chi \cos 2\psi \\ S_0 \cos 2\chi \sin 2\psi \\ S_0 \sin 2\psi \end{bmatrix}$$

Wave Polarizations: Geometrical Representations

Polarization Ellipse

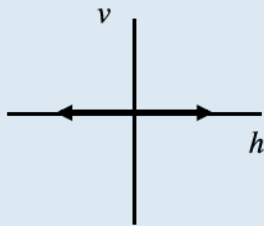


Poincaré Sphere



Example Polarizations

Linear Horizontal

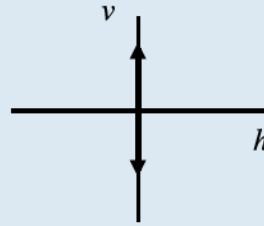


$$\vec{p} = \begin{bmatrix} 1 \\ 0 \end{bmatrix}$$

$$\psi = 0^\circ, \chi = 0^\circ$$

$$\vec{S} = \begin{bmatrix} 1 \\ 1 \\ 0 \\ 0 \end{bmatrix}$$

Linear Vertical

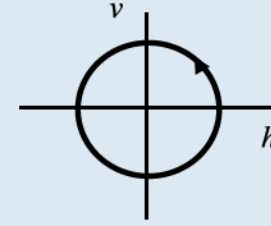


$$\vec{p} = \begin{bmatrix} 0 \\ 1 \end{bmatrix}$$

$$\psi = 90^\circ, \chi = 0^\circ$$

$$\vec{S} = \begin{bmatrix} 1 \\ -1 \\ 0 \\ 0 \end{bmatrix}$$

Left-hand Circular



$$\vec{p} = \frac{1}{\sqrt{2}} \begin{bmatrix} 1 \\ -i \end{bmatrix}$$

$$\psi = 0^\circ, \chi = 45^\circ$$

$$\vec{S} = \begin{bmatrix} 1 \\ 0 \\ 0 \\ 1 \end{bmatrix}$$

Scattering Matrix and Radar Cross Section

- The amount of signal returned by the radar depends on the physics of the interaction of microwaves with the surface.
- The physics of the scattered field is encoded in the *scattering matrix* (Sinclair Matrix) that relates the scattered and incident fields.

$$\vec{E}^s = \begin{bmatrix} E_h^s \\ E_v^s \end{bmatrix} = \begin{bmatrix} S_{hh} & S_{hv} \\ S_{vh} & S_{vv} \end{bmatrix} \begin{bmatrix} E_h^i \\ E_v^i \end{bmatrix}$$

- Radar Cross Section (RCS) $\sigma_{pq} = 4\pi |S_{pq}|^2$

- Normalized (RCS) or Backscatter $\sigma_{pq}^o = \frac{\sigma_{pq}}{A_g}$

A_g is ground area within a resolution element

- Gamma $\gamma_{pq}^o = \frac{\sigma_{pq}^o}{\cos \theta_i}$

Basic Scattering Mechanisms

- Thin conducting cylinder (horizontal)

$$S = \begin{bmatrix} a & 0 \\ 0 & 0 \end{bmatrix} \quad \text{At } 45^\circ, \quad S = \begin{bmatrix} a & -a \\ -a & a \end{bmatrix}$$

- Surface scattering (Bragg) : $b > a$

$$\begin{bmatrix} S_{HH} & S_{HV} \\ S_{VH} & S_{VV} \end{bmatrix} = \begin{bmatrix} a & 0 \\ 0 & b \end{bmatrix}$$

- Dihedral - conducting

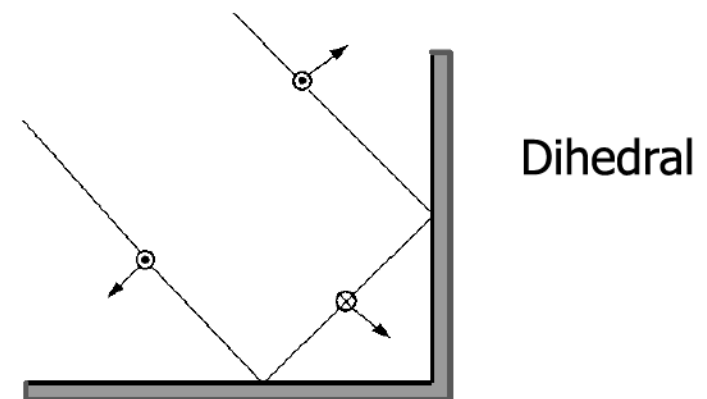
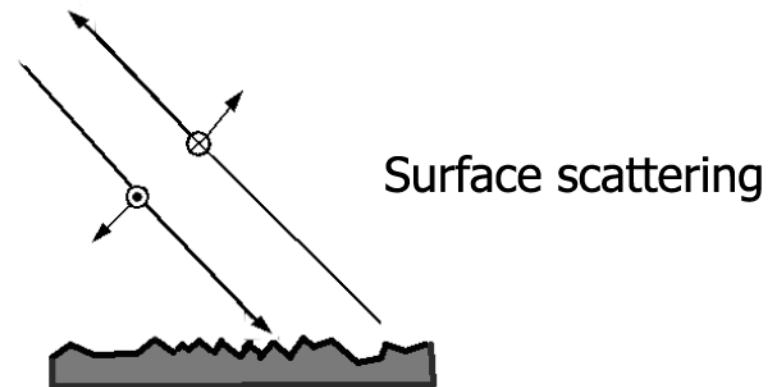
$$\begin{bmatrix} S_{HH} & S_{HV} \\ S_{VH} & S_{VV} \end{bmatrix} = \begin{bmatrix} a & 0 \\ 0 & -a \end{bmatrix}$$

- HH and VV phase difference = 180°

- o Non-conducting surface $< 180^\circ$

- Round trip distance identical

- Strong return

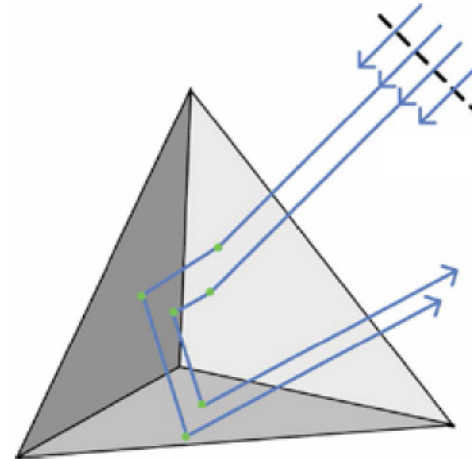


Trihedral Scattering

- For a trihedral reflector:

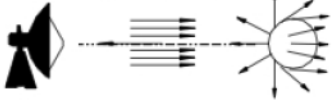
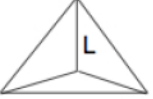
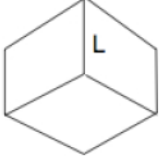
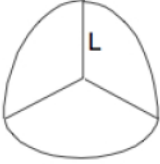
$$\begin{bmatrix} S_{HH} & S_{HV} \\ S_{VH} & S_{VV} \end{bmatrix} = \begin{bmatrix} a & 0 \\ 0 & a \end{bmatrix}$$

- HH and VV phase difference = 0°
- Useful for calibration
- Beamwidth independent of wavelength



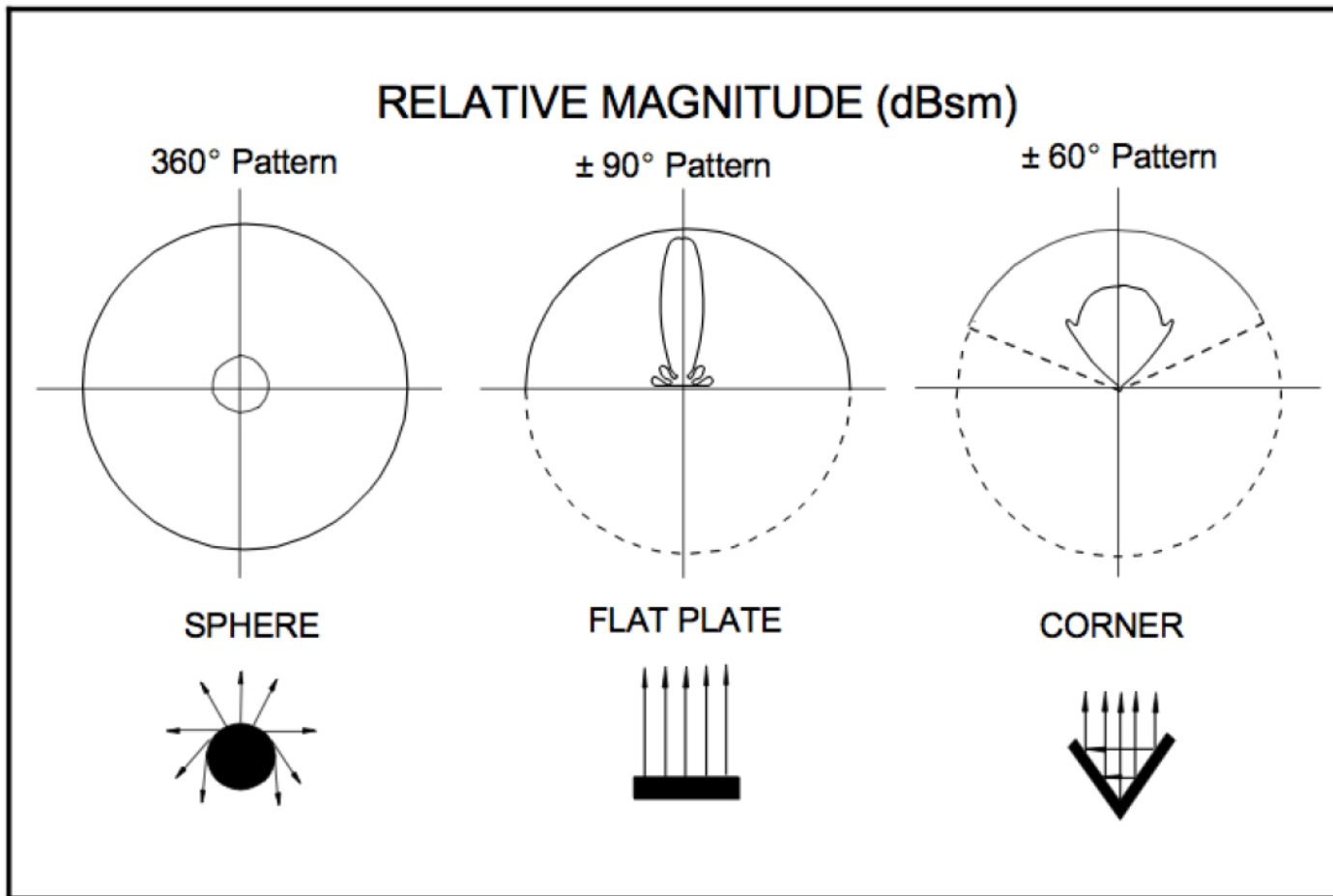
RCS of Some Standard Objects

- The RCS of many objects varies as the inverse of the wavelength squared
- Larger wavelength require larger reflectors to have the same cross section.

<p>SPHERE</p>  <p>$\sigma_{\max} = \pi r^2$</p>	<p>CORNER</p> 
<p>CYLINDER</p>  <p>$\sigma_{\max} = \frac{2\pi r h^2}{\lambda}$</p>	<p>$\sigma_{\max} = \frac{8\pi w^2 h^2}{\lambda^2}$</p>  <p>Dihedral Corner Reflector</p>
<p>FLAT PLATE</p>  <p>$\sigma_{\max} = \frac{4\pi w^2 h^2}{\lambda^2}$</p>	<p>$\sigma_{\max} = \frac{4\pi L^4}{3\lambda^2}$</p> 
<p>TILTED PLATE</p>  <p>Same as above for what reflects away from the plate and could be zero reflected to radar</p>	<p>$\sigma_{\max} = \frac{12\pi L^4}{\lambda^2}$</p>  <p>$\sigma_{\max} = \frac{15.6\pi L^4}{3\lambda^2}$</p>  <p>Trihedral Corner Reflectors</p>

RCS Patterns

The RCS is in general angularly dependent





Scattering Matrix

- The radiated and scattered electric fields are related through the complex 2x2 scattering matrix:

$$\vec{E}^s = [S] \vec{p}^{rad}$$

- The (complex) voltage measured at the antenna terminals is given by the scalar product of the receiving antenna polarization vector and the received wave electric field:

$$V_m = \langle \vec{p}^{rec}, [S] \vec{p}^{rad} \rangle$$

- The measured power is the magnitude of the (complex) voltage squared:

$$P_m = V_m V_m^* = |\langle \vec{p}^{rec}, [S] \vec{p}^{rad} \rangle|^2$$

NOTE: Radar cross-section is proportional to power

Vector Formulation of Polarimetric Returns

- For 2 x 2 complex matrices:
$$A = \begin{bmatrix} a_{11} & a_{12} \\ a_{21} & a_{22} \end{bmatrix}, \quad B = \begin{bmatrix} b_{11} & b_{12} \\ b_{21} & b_{22} \end{bmatrix}$$
- Define the Matrix Inner Product: $A \bullet B = \text{trace}(B^\dagger A)$
- The inner product corresponds to the standard complex inner product if we arrange the matrix elements in a 4-element complex vector

$$\vec{A} \bullet \vec{B} = \begin{bmatrix} b_{11}^* & b_{12}^* & b_{21}^* & b_{22}^* \end{bmatrix} \begin{bmatrix} a_{11} \\ a_{12} \\ a_{21} \\ a_{22} \end{bmatrix}$$

$$= a_{11} b_{11}^* + a_{21} b_{21}^* + a_{12} b_{12}^* + a_{22} b_{22}^*$$

$$B^\dagger A = \begin{bmatrix} a_{11} b_{11}^* + a_{21} b_{21}^* & a_{12} b_{11}^* + a_{22} b_{21}^* \\ a_{11} b_{12}^* + a_{21} b_{22}^* & a_{12} b_{12}^* + a_{22} b_{22}^* \end{bmatrix}$$

$$\text{Trace}(B^\dagger A) = a_{11} b_{11}^* + a_{21} b_{21}^* + a_{12} b_{12}^* + a_{22} b_{22}^*$$

Standard Basis Matrices

- The Standard Polarization basis, S_p , are a set orthogonal matrices

$$S_p = \left\{ \begin{bmatrix} 1 & 0 \\ 0 & 0 \end{bmatrix}, \begin{bmatrix} 0 & 1 \\ 0 & 0 \end{bmatrix}, \begin{bmatrix} 0 & 0 \\ 1 & 0 \end{bmatrix}, \begin{bmatrix} 0 & 0 \\ 0 & 1 \end{bmatrix} \right\}$$

- For

$$S = \begin{bmatrix} S_{HH} & S_{HV} \\ S_{VH} & S_{VV} \end{bmatrix}$$

- Projecting S onto the Standard Basis elements we can form an equivalent scattering vector \vec{k}

$$\vec{k} = \text{trace}(SS_p) = \begin{bmatrix} \text{trace}(SS_1) \\ \text{trace}(SS_2) \\ \text{trace}(SS_3) \\ \text{trace}(SS_4) \end{bmatrix} = \begin{bmatrix} S_{HH} \\ S_{HV} \\ S_{VH} \\ S_{VV} \end{bmatrix}$$

Covariance Matrix

- For backscattering geometries in a reciprocal medium where reciprocity applies, $S_{HV} = S_{VH}$ and the 4-dimensional vector can be projected in a 3-dimensional subspace where we take 2nd basis element to be the unit vector formed by the linear combination of the 2nd and 3rd elements

$$proj(\vec{k}) = \vec{k}_s = \frac{1}{2} \begin{bmatrix} trace(SS_1) \\ trace\left(S \frac{1}{\sqrt{2}} (S_2 + S_3)\right) \\ trace(SS_4) \end{bmatrix} = \begin{bmatrix} S_{HH} \\ \sqrt{2}S_{HV} \\ S_{VV} \end{bmatrix}$$

- The associated covariance matrix is

$$Z = \vec{k}_s \vec{k}_s^\dagger = \begin{bmatrix} \langle |S_{HH}|^2 \rangle & \sqrt{2} \langle S_{HH} S_{HV}^* \rangle & \langle S_{HH} S_{VV}^* \rangle \\ \sqrt{2} \langle S_{HV} S_{HH}^* \rangle & 2 \langle |S_{HV}|^2 \rangle & \sqrt{2} \langle S_{HV} S_{VV}^* \rangle \\ \langle S_{VV} S_{HH}^* \rangle & \sqrt{2} \langle S_{VV} S_{HV}^* \rangle & \langle |S_{VV}|^2 \rangle \end{bmatrix}$$

Pauli Basis Matrices

- The Pauli Basis matrices, Ψ_p , are a set of orthogonal matrices
- This basis is particularly useful due to the physical interpretability of basic polarimetric scattering mechanisms when expressed using this basis

$$\Psi_p = \left\{ \sqrt{2} \begin{bmatrix} 1 & 0 \\ 0 & 1 \end{bmatrix}, \sqrt{2} \begin{bmatrix} 1 & 0 \\ 0 & -1 \end{bmatrix}, \sqrt{2} \begin{bmatrix} 0 & 1 \\ 1 & 0 \end{bmatrix}, \sqrt{2} \begin{bmatrix} 0 & -i \\ i & 0 \end{bmatrix} \right\}$$

- Projecting S onto the Pauli Basis elements we can form an equivalent scattering vector \vec{k}

$$\vec{k} = \frac{1}{2} \text{trace}(S\Psi_p) = \frac{1}{2} \begin{bmatrix} \text{trace}(SP_1) \\ \text{trace}(SP_2) \\ \text{trace}(SP_3) \\ \text{trace}(SP_4) \end{bmatrix} = \frac{1}{\sqrt{2}} \begin{bmatrix} S_{HH} + S_{VV} \\ S_{HH} + S_{VV} \\ S_{HV} + S_{VH} \\ i(S_{HV} - S_{VH}) \end{bmatrix}$$

Coherency Matrix

- For backscattering geometries in a reciprocal medium where reciprocity applies, $S_{HV} = S_{VH}$ and the 4-dimensional vector can be projected in a 3-dimensional subspace.

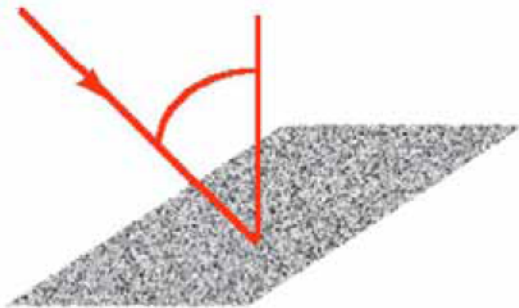
$$proj(\vec{k}) = \vec{k}_{HV} = \frac{1}{2} \begin{bmatrix} trace(SP_1) \\ trace(SP_2) \\ trace(SP_3) \end{bmatrix} = \frac{1}{\sqrt{2}} \begin{bmatrix} S_{HH} + S_{VV} \\ S_{HH} - S_{VV} \\ 2S_{HV} \end{bmatrix}$$

- The associated coherency matrix is

$$T = \vec{k}_{HV} \vec{k}_{HV}^\dagger = \frac{1}{2} \begin{bmatrix} \langle |S_{HH} + S_{VV}|^2 \rangle & \langle (S_{HH} + S_{VV})(S_{HH} - S_{VV})^* \rangle & 2\langle (S_{HH} + S_{VV})S_{HV}^* \rangle \\ \langle (S_{HH} - S_{VV})(S_{HH} + S_{VV})^* \rangle & \langle |S_{HH} - S_{VV}|^2 \rangle & 2\langle (S_{HH} - S_{VV})S_{HV}^* \rangle \\ 2\langle (S_{HH} + S_{VV})S_{HH}^* \rangle & 2\langle (S_{HH} - S_{VV})S_{HV}^* \rangle & 4\langle |S_{HV}|^2 \rangle \end{bmatrix}$$

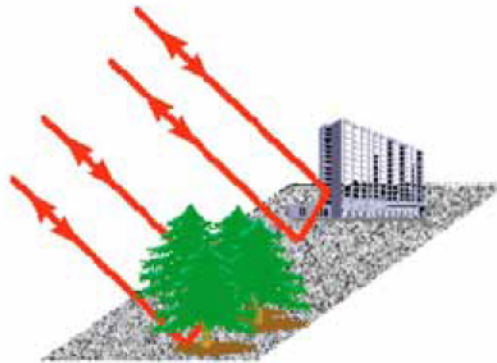
Target Generators - Physical Interpretation

Single Bounce
Scattering
(Rough Surface)



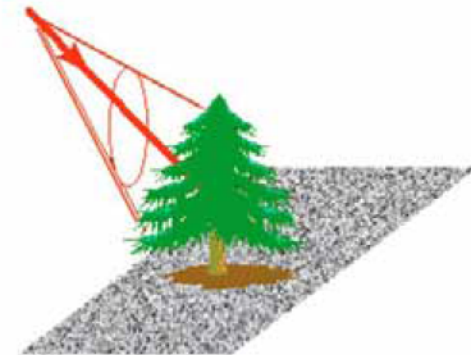
$$T_{11} = \frac{1}{2} |S_{HH} + S_{VV}|^2$$

Double Bounce
Scattering



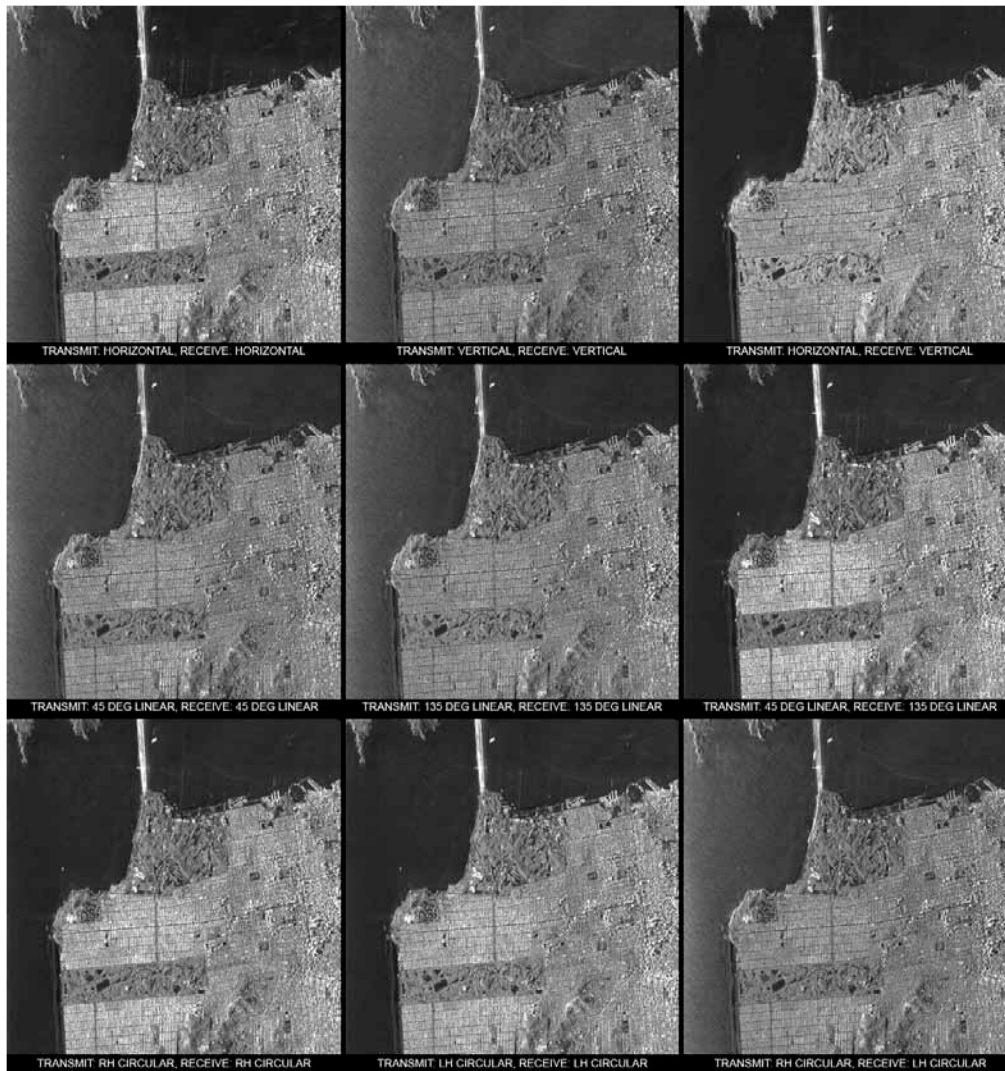
$$T_{22} = \frac{1}{2} |S_{HH} - S_{VV}|^2$$

Volume
Scattering



$$T_{33} = 2 |S_{HV}|^2$$

Image Intensity for Selected Polarizations



- View of San Francisco for various polarizations.
- Different land cover types respond differently to different polarizations.
- This diversity can be exploited both in classifications and quantitative surface parameter determination.

Utility of the Covariance Matrix

$$\begin{aligned}
 V_m &= \vec{p}^{\text{rec}} [S] \vec{p}^{\text{rad}} \\
 &= p_h^{\text{rec}} p_h^{\text{rad}} S_{hh} + p_h^{\text{rec}} p_v^{\text{rad}} S_{hv} + p_v^{\text{rec}} p_h^{\text{rad}} S_{vh} + p_v^{\text{rec}} p_v^{\text{rad}} S_{vv} \\
 &= p_h^{\text{rec}} p_h^{\text{rad}} S_{hh} + 2p_h^{\text{rec}} p_v^{\text{rad}} S_{hv} + p_v^{\text{rec}} p_v^{\text{rad}} S_{vv} \\
 &= \begin{bmatrix} p_h^{\text{rec}} p_h^{\text{rad}} & \sqrt{2} p_h^{\text{rec}} p_v^{\text{rad}} & p_v^{\text{rec}} p_v^{\text{rad}} \end{bmatrix} \begin{bmatrix} S_{hh} \\ \sqrt{2} S_{hv} \\ S_{vv} \end{bmatrix} = \vec{A}^t \vec{k}
 \end{aligned}$$

- The first vector contains only antenna parameters, while the second contains only scattering matrix elements. Using this expression in the power expression, one finds

$$P_m = V_m V_m^* = (\vec{A}^t \vec{k})(\vec{A}^t \vec{k})^* = (\vec{A}^t \vec{k})(\vec{k}^\dagger \vec{A}^*) = \vec{A}^t (\vec{k} \vec{k}^\dagger) \vec{A}^*$$

- where the covariance matrix $Z = \vec{k} \vec{k}^\dagger$ defined previously shows up in the expression for the power.



Another way to Compute Power: Stokes Scattering Operator

- If the fields are represented by Stokes vectors, then it can be shown that there is a matrix that allows one to calculate the power as with the covariance matrix:

$$P_m = \begin{bmatrix} 1 & \cos 2\psi_r \cos 2\chi_r & \sin 2\psi_r \cos 2\chi_r & \sin 2\chi_r \end{bmatrix} \begin{bmatrix} m_{11} & m_{12} & m_{13} & m_{14} \\ m_{21} & m_{22} & m_{23} & m_{24} \\ m_{31} & m_{32} & m_{33} & m_{34} \\ m_{41} & m_{42} & m_{43} & m_{44} \end{bmatrix} \begin{bmatrix} 1 \\ \cos 2\psi_t \cos 2\chi_t \\ \sin 2\psi_t \cos 2\chi_t \\ \sin 2\chi_t \end{bmatrix}$$

- With this expression, once the elements of M are calculated for a particular scatterer, the received power can be described in terms of the polarization state of the transmitter and receiver
- The representation of M in terms of S_{XY} is messy, however is simple for certain canonical targets, like corner reflectors.

Polarimetric Response of a Trihedral CR

- For the simple case of a trihedral corner reflector, the power expressing becomes:

$$P_m = \begin{bmatrix} 1 & \cos 2\psi_r \cos 2\chi_r & \sin 2\psi_r \cos 2\chi_r & \sin 2\chi_r \end{bmatrix} \begin{bmatrix} a^2 & 0 & 0 & 0 \\ 0 & a^2 & 0 & 0 \\ 0 & 0 & a^2 & 0 \\ 0 & 0 & 0 & -a^2 \end{bmatrix} \begin{bmatrix} 1 \\ \cos 2\psi_t \cos 2\chi_t \\ \sin 2\psi_t \cos 2\chi_t \\ \sin 2\chi_t \end{bmatrix}$$

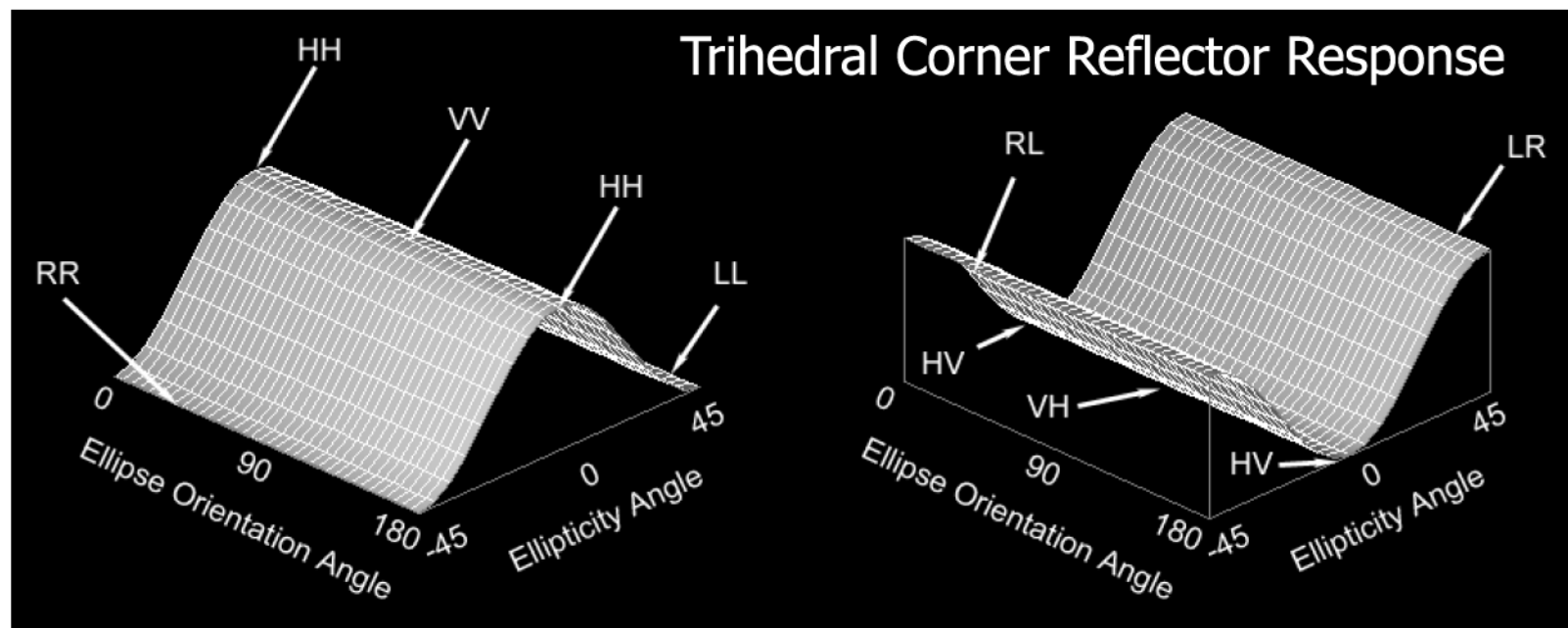
which reduces to

$$P_m = a^2 (1 \pm \cos 4\chi)$$

- + for co-polarized transmit and receive
- for cross-polarized transmit and receive

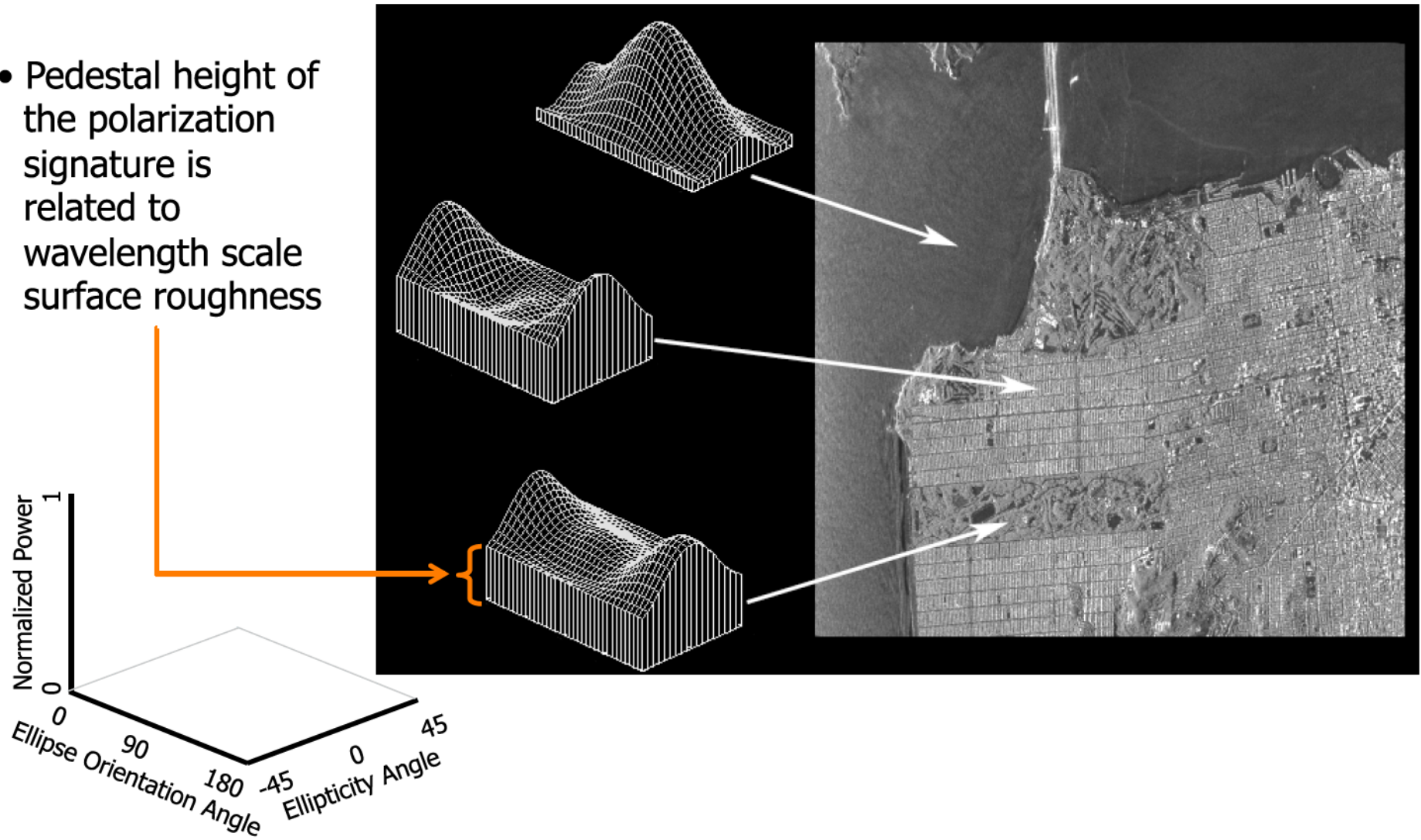
Basic Tools: Polarization Signature

- The polarization signature is a graphical way to display the radar cross-section as a function of polarization
- Usually co- and cross-polarization signatures are displayed together



Co-Polarization Signatures of San Francisco

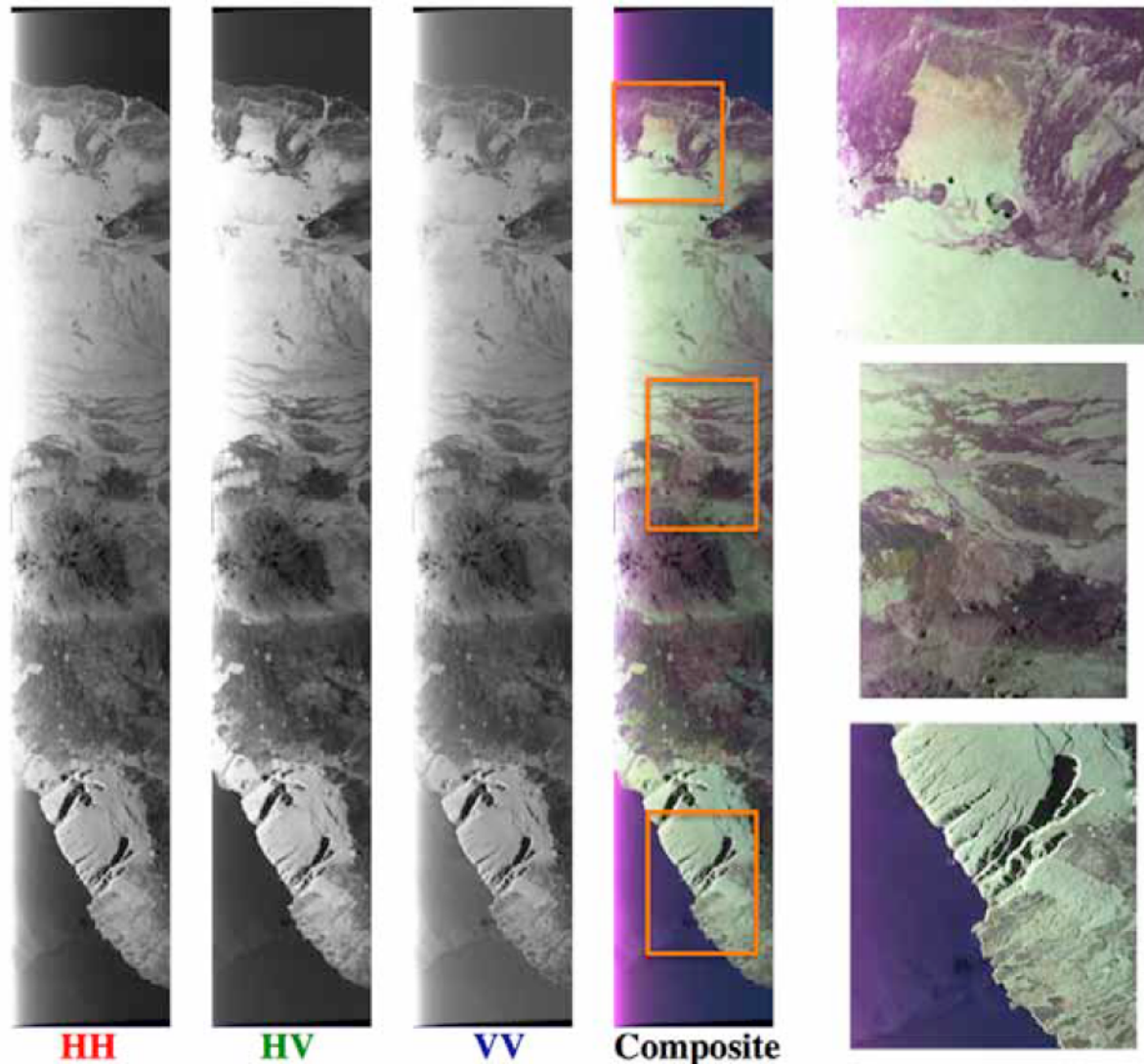
- Pedestal height of the polarization signature is related to wavelength scale surface roughness



Color Composite UAVSAR Polarimetric Image

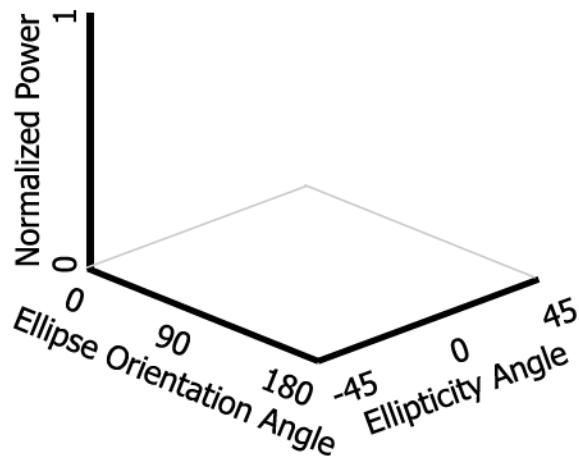
Polarimetric image of the Big Island of Hawaii

Vegetation appears light green because HV signal dominates as multiple scattering in canopy depolarizes transmitted signal on backscatter

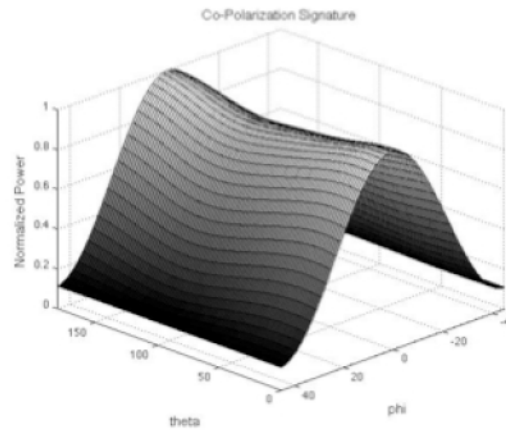


UAVSAR Co-Polarization Signatures

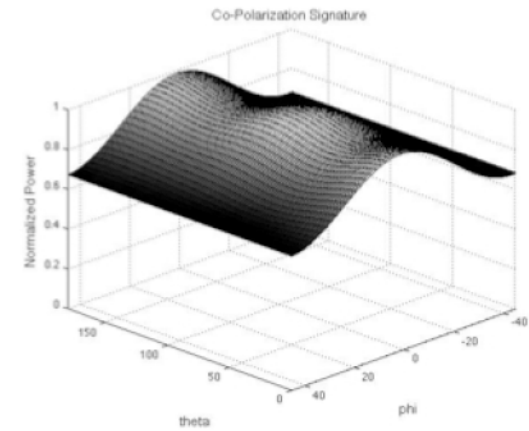
Pedestal height can often be linked to the amount of surface roughness and the shape and number of peaks provide insight into the scattering mechanism involved.



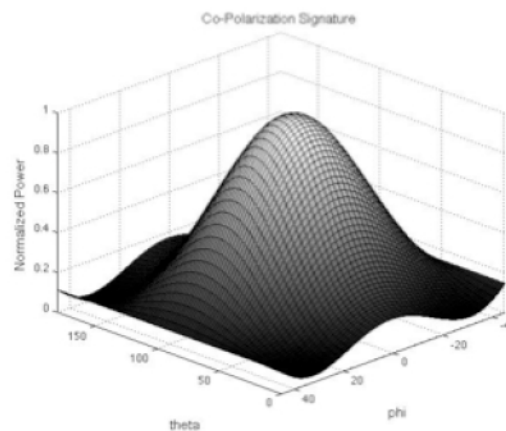
Lava



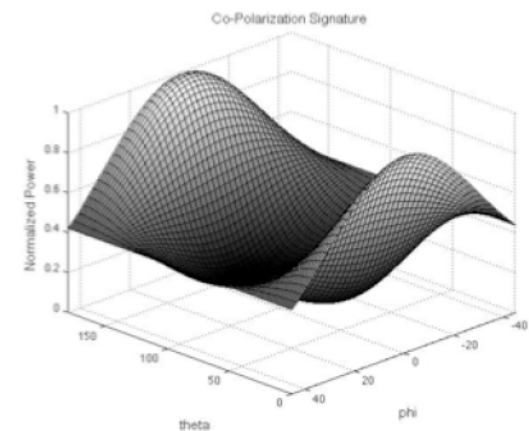
Forest



Ocean



Building



Eigenvalue Decomposition

- Cloude showed that a general polarimetric covariance or coherency matrix can be decomposed as follows:

$$\vec{T} = \sum_{k=1}^3 \lambda_i \vec{k}_i \vec{k}_i^\dagger$$

- Here, λ_i , $i=1,3$ are the eigenvalues of the covariance matrix, \vec{k}_i are its eigenvectors.
- For terrain with reflection symmetry, the eigenvectors can be interpreted to represent odd numbers of reflection, even numbers of reflection and diffuse scattering
- The eigenvalues and eigenvectors of the covariance have been combined in many ways to provide various physical interpretations of the scattering processes present in a polarimetric image.

Polarimetric Measures of Randomness

Polarimetric Entropy

$$H_T = -\sum_{i=1}^3 P_i \log_3 P_i; \quad P_i = \frac{\lambda_i}{\lambda_1 + \lambda_2 + \lambda_3}$$

Alpha Angle

$$\underline{\alpha} = \sum_{i=1}^3 P_i \alpha_i; \quad \alpha_i = \cos^{-1} k_{i1}$$

Pedestal Height

$$\text{Pedestal Height} = \frac{\min(\lambda_1, \lambda_2, \lambda_3)}{\max(\lambda_1, \lambda_2, \lambda_3)}$$

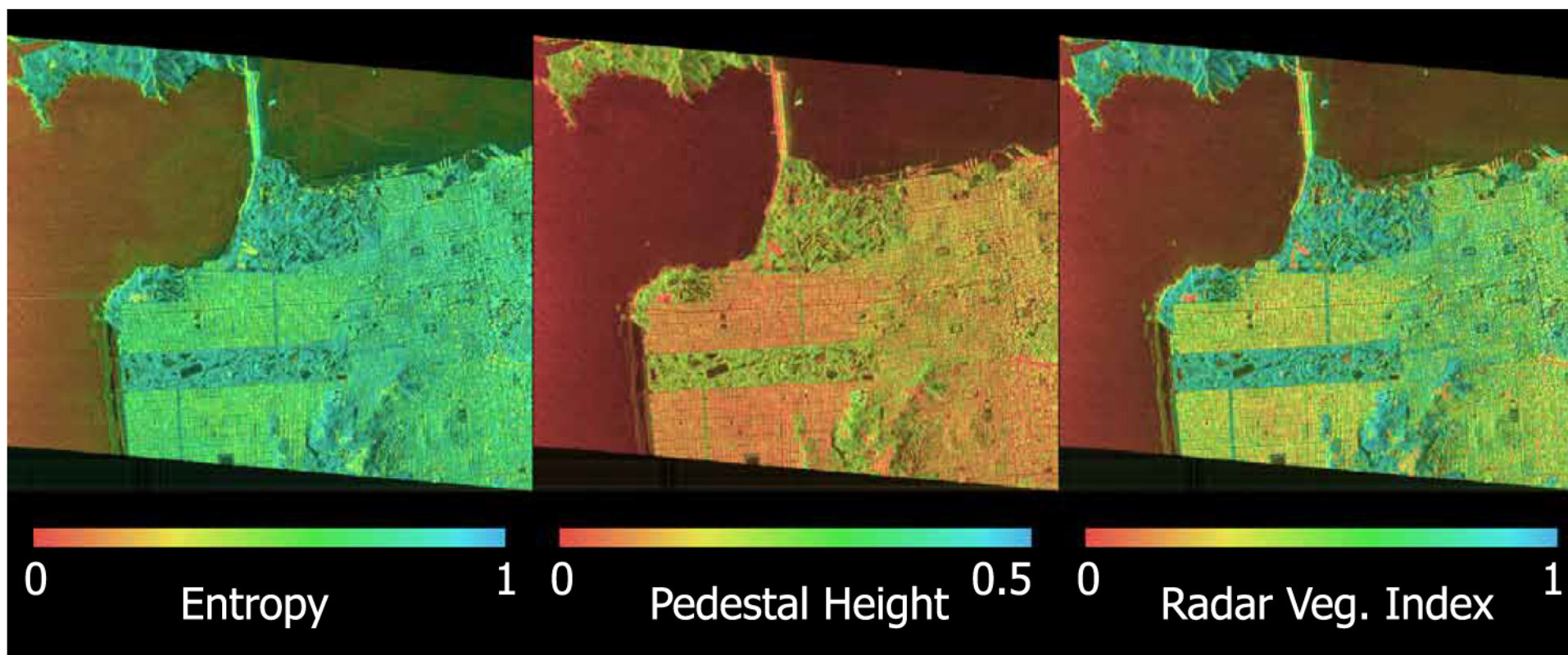
Eigenvalues λ_i and eigenvectors k_i derived from eigenvalue decomposition of coherency matrix

Radar Vegetation Index

$$RVI = \frac{4 \min(\lambda_1, \lambda_2, \lambda_3)}{\lambda_1 + \lambda_2 + \lambda_3} = \frac{8\sigma_{hv}}{\sigma_{hh} + \sigma_{vv} + 2\sigma_{hv}}$$

Polarimetric Randomness

San Francisco, California

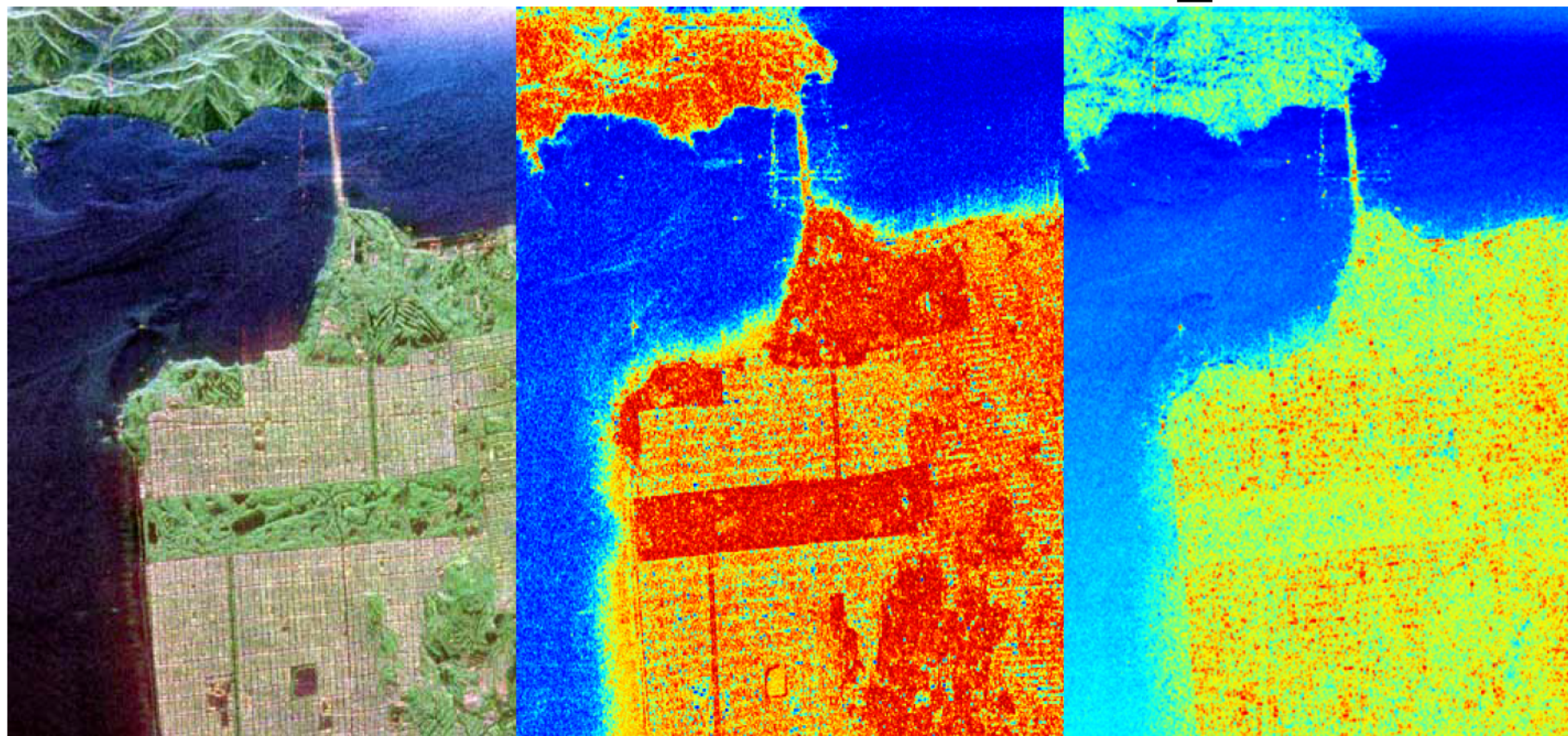


H / A / α Decomposition

IMAGE

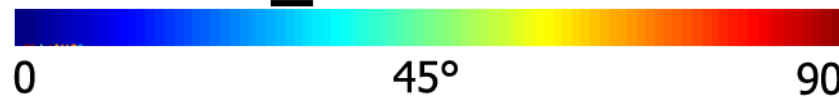
ENTROPY

α PARAMETER



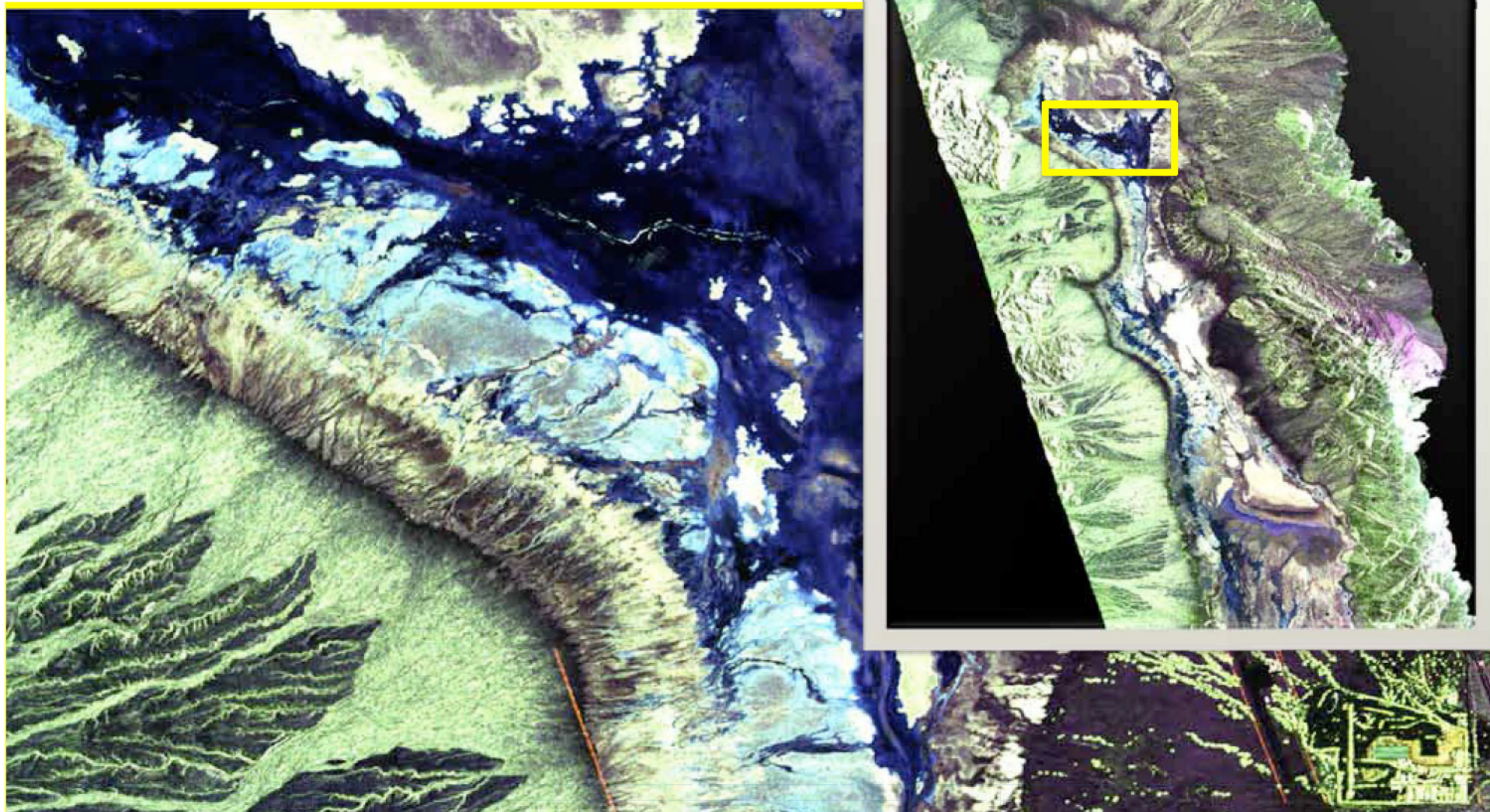
ENTROPY (H)

α PARAMETER



Polarimetric SAR at Death Valley

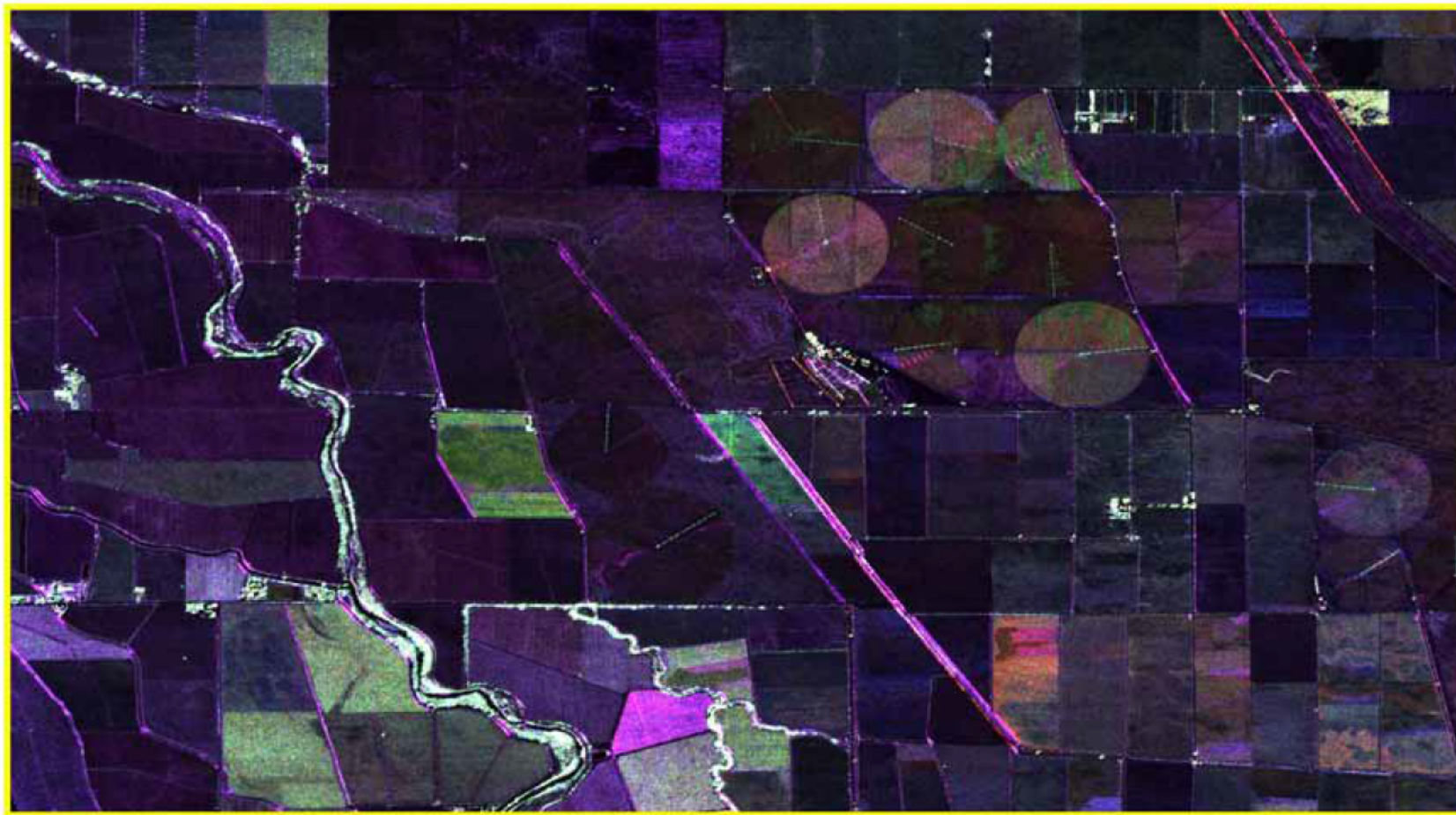
HH-Red HV – Green VV – Blue



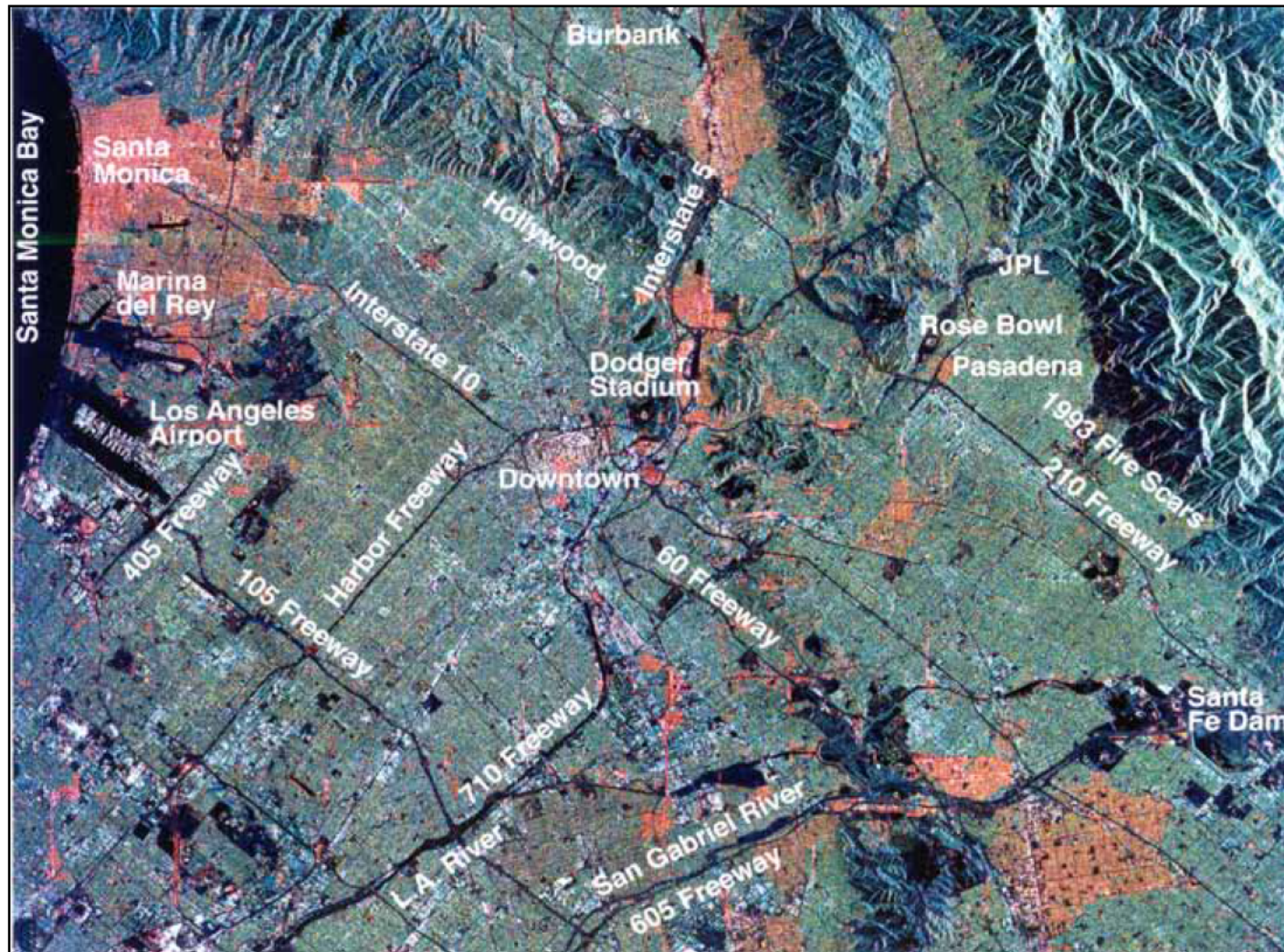
San Joaquin Valley, California

Applications: soil moisture estimation,
vegetation classification

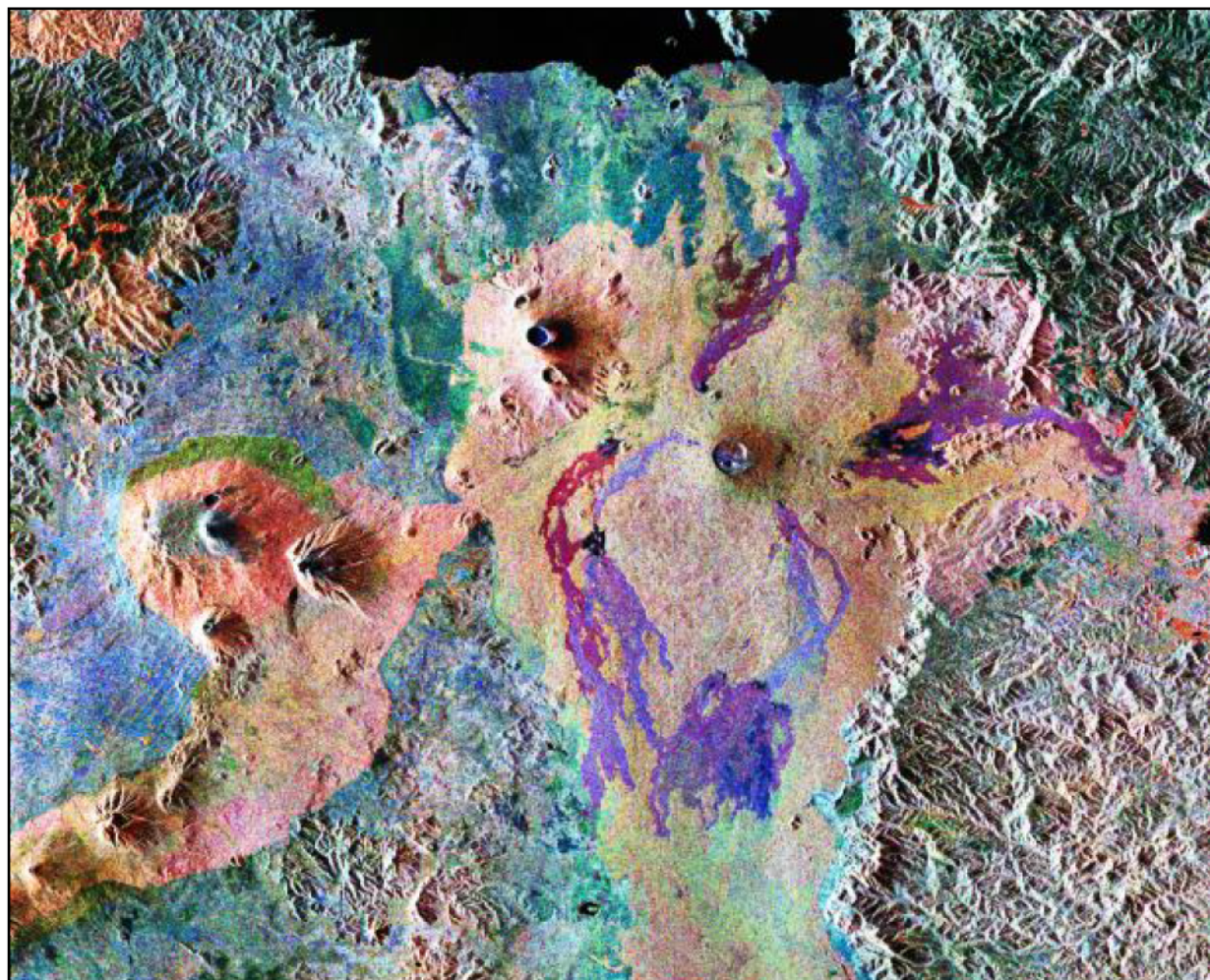
HH-Red HV – Green VV – Blue



Polarimetry from SIR-C/X-SAR



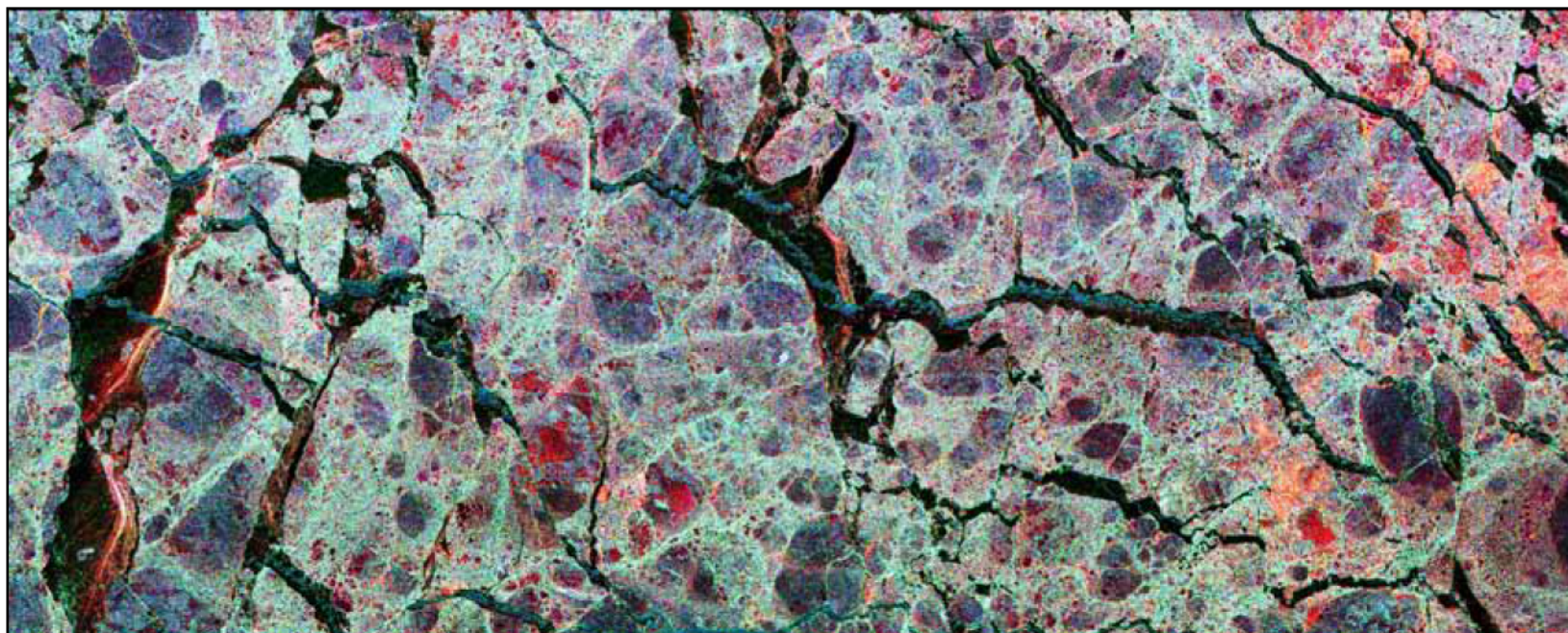
SIR-C/X-SAR: Characterizing the Earth's Surface



Volcanoes

SIR-C/X-SAR Views Sea Ice

Multi-frequency, multi-polarization radar can measure the extent, thickness and morphology of the polar ice pack.



Red: CHH Green: LHV Blue: LHH

Weddell Sea, Antarctica

Gallery of JPL Missions

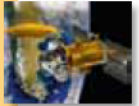


Grail
Sep 2011
Moon Gravity



Juno
August 2011
Jupiter

Aquarius/SAC-D
June 2011
Sea Salinity



Also:

GaleX
2003

MM
2008

Divi
2009

Kepler
2009

Herschel
2009



Explorer 1-5
1958
Van Allen Belts



Ulysses
1990
Solar Polar Orbit



Microwave Instrument
2004
Rosetta Comet Orbiter



MARSIS
2003
Deep Sounder

Spitzer Telescope
2003
Infrared Telescope



Seawinds
2002
Ocean Winds



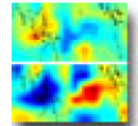
Pioneer 3-4
1958
Lunar Flybys



Wide Field Camera
1990
Fix Hubble



Emission Spectrometer
2004
Infrared Sensor



Microwave Sounder
2004
Ozone

Mars Rovers
2003
Rovers



Genesis
2001
Solar Wind Samples



Rangers
1961-1965
Lunar Surveys



Topex/Poseidon
1992
Ocean Altimeter



Global Surveyor
1996
Mars Orbiter



SRTM
2000
Earth Radar



Surveyors
1966-1968
Lunar Landers



Cassini
1997
Saturn & Moons



Deep Impact
2005
Smash Comet EPOXI



MRO
2005
SHARAD



Cloudsat
2006
Precipitation

Grace
2002
Earth Gravity



Deep Space 1
1998
Ion Engine



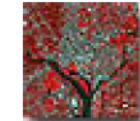
Mariner 1-2
1962
Venus Flybys



Stardust
1999
Comet Wild-2



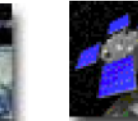
Quickscat
1999
Sea Winds



Radiometer
1999
Earth Thermal



Multi-Angle Spect
1999
Earth Imaging



Active Cavity
1999
Solar Radiance



Keck
2001
Astronomy



Jason 1
2001
Ocean Altimetry

VLBI
1997
Astronomy



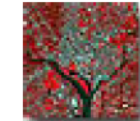
Mariner 3-4
1964
Mars Flybys



Stardust
1999
Comet Wild-2



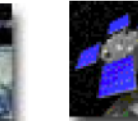
Quickscat
1999
Sea Winds



Radiometer
1999
Earth Thermal



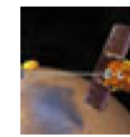
Multi-Angle Spect
1999
Earth Imaging



Active Cavity
1999
Solar Radiance



Keck
2001
Astronomy



Mars Odyssey
2001
Mars Imaging

Pathfinder
1996
Mars Rover



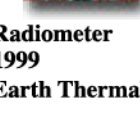
Mariner 5
1967
Venus Flyby



Stardust
1999
Comet Wild-2



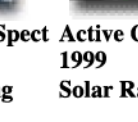
Quickscat
1999
Sea Winds



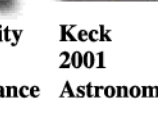
Radiometer
1999
Earth Thermal



Multi-Angle Spect
1999
Earth Imaging



Active Cavity
1999
Solar Radiance



Keck
2001
Astronomy



Mars Odyssey
2001
Mars Imaging

NSCAT
1996
Earth Winds



Mariner 6-7
1969
Mars Flybys



Mariner 8-9
1971
Mars Orbiter



Mariner 10
1973
Venus / Merc



Viking
1975
Mars Landers



Voyager
1977
Grand Tour



Seasat
1978
Earth Radar



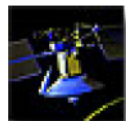
Solar Explorer
1981
Earth Ozone



SIR A, B, C
1981, 84, 94
Earth Radar



Infrared Sat
1983
Telescope



Magellan
1989
Venus Radar



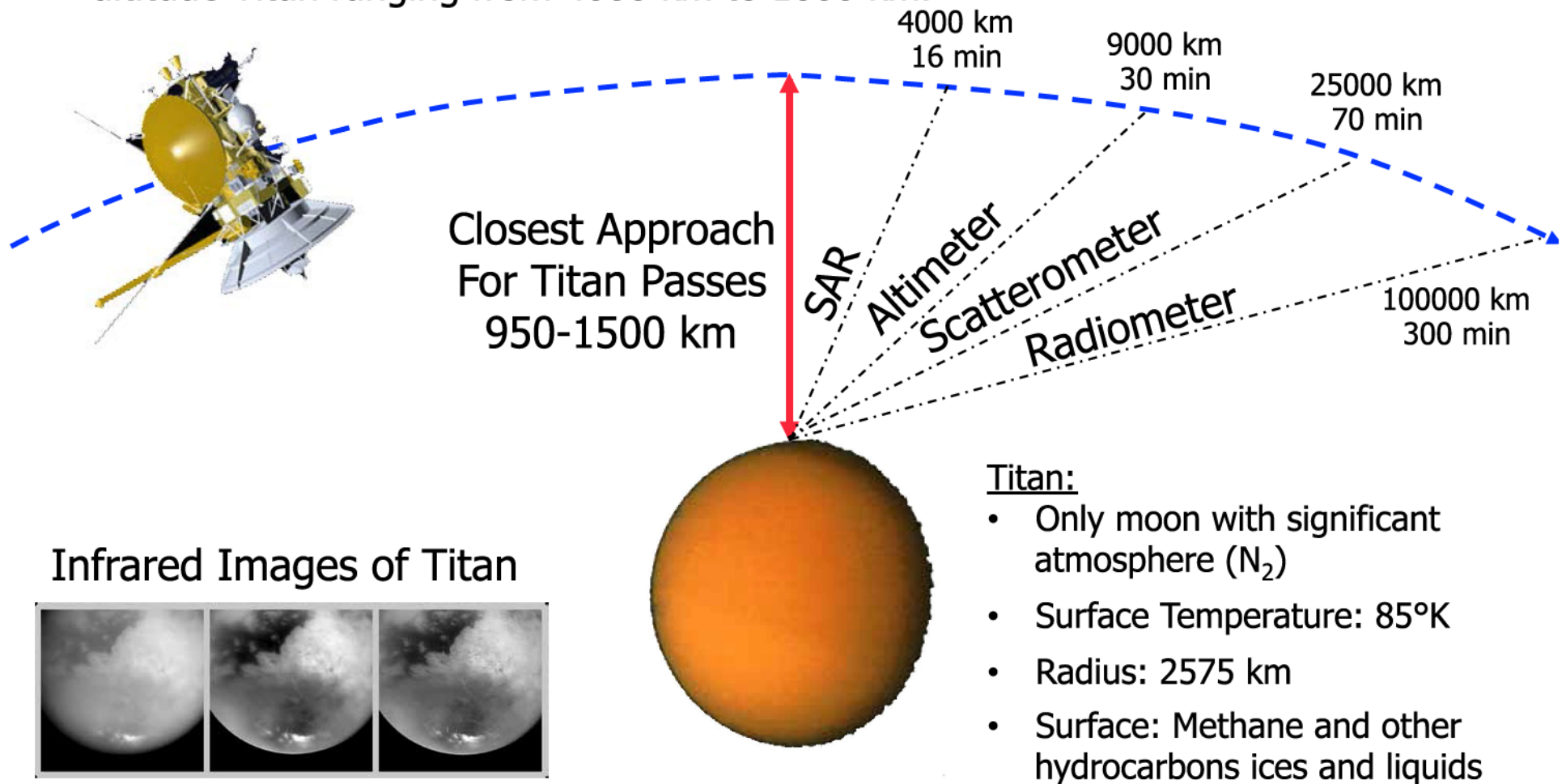
Galileo
1989
Jupiter



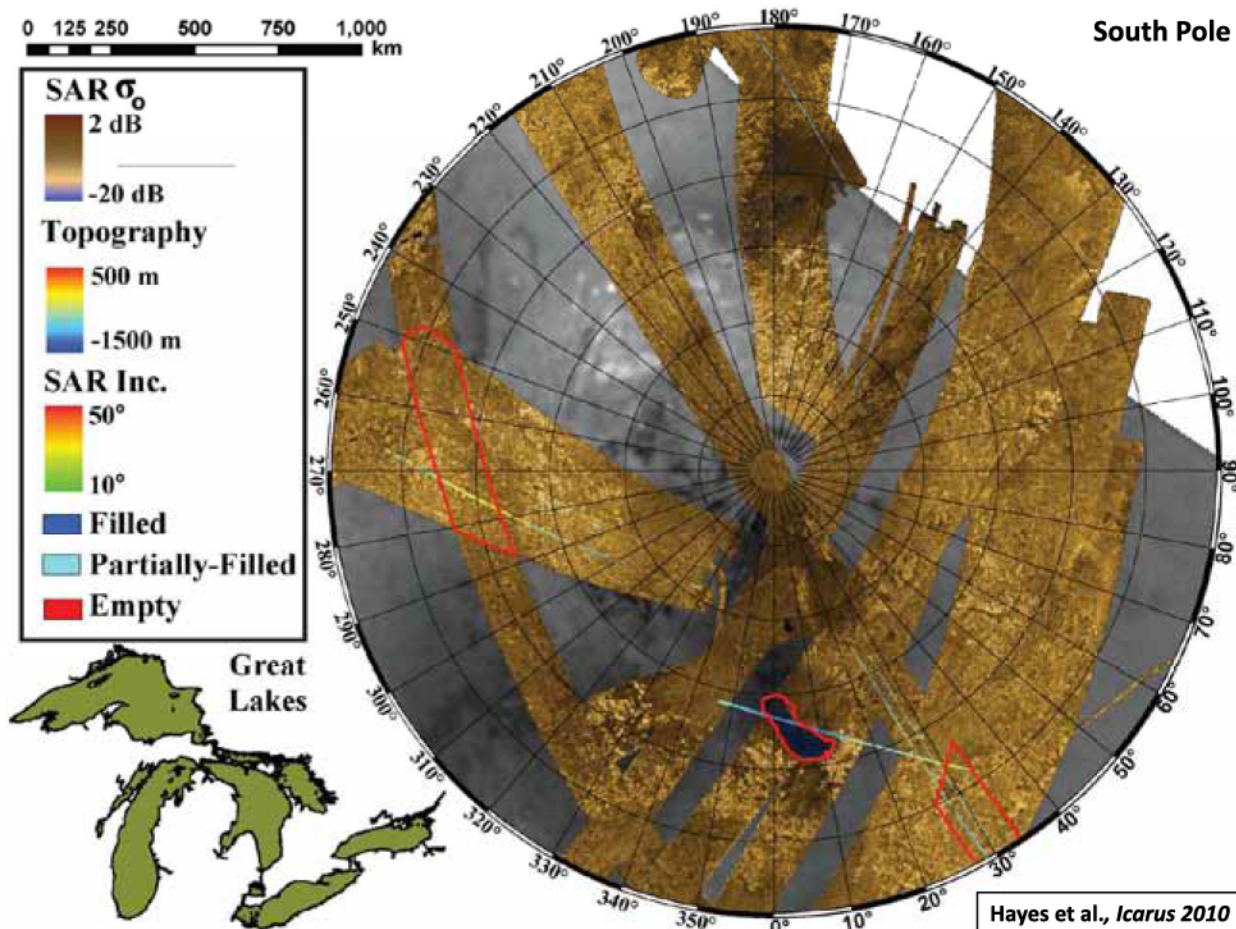
Mars Observer
1992
Mars Orbiter

Titan Observation Geometry

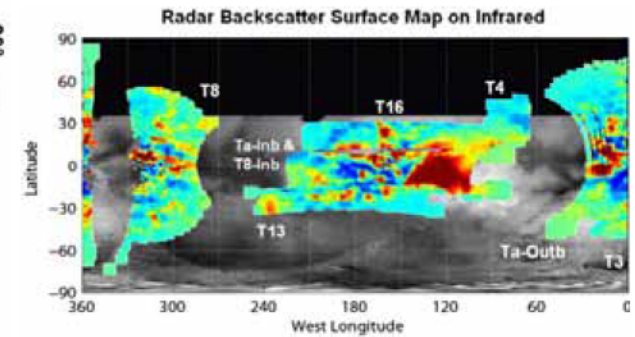
SAR imaging takes place from around ± 16 minutes from closest approach with altitude Titan ranging from 4000 km to 1000 km.



Cassini Radar Results



(Courtesy S. Hensley)



Wye et al. (*Icarus*, 2007)



Summary

- This lecture was just a taste of radar remote sensing techniques and applications. Other important areas include
 - Stereo radargrammetry
 - PolInSAR for volumetric structure mapping
 - Agricultural monitoring, soil moisture, ice-mapping, ...
- The broad range of sensor types, frequencies of observation and availability of sensors have enabled radar sensors to make significant contributions in a wide area of earth and planetary remote sensing sciences
- The range of applications, both qualitative and quantitative, continue to expand with each new generation of sensors